

Ultrafast Imaging in Biomedical Ultrasound

Mickael Tanter and Mathias Fink

Abstract—Although the use of ultrasonic plane-wave transmissions rather than line-per-line focused beam transmissions has been long studied in research, clinical application of this technology was only recently made possible through developments in graphical processing unit (GPU)-based platforms. Far beyond a technological breakthrough, the use of plane or diverging wave transmissions enables attainment of ultrafast frame rates (typically faster than 1000 frames per second) over a large field of view. This concept has also inspired the emergence of completely novel imaging modes which are valuable for ultrasound-based screening, diagnosis, and therapeutic monitoring. In this review article, we present the basic principles and implementation of ultrafast imaging. In particular, present and future applications of ultrafast imaging in biomedical ultrasound are illustrated and discussed.

I. ACOUSTICS, OPTICAL HOLOGRAPHY, AND TIME REVERSAL

CONVENTIONAL ultrasonography for medical ultrasound emerged in the 1970s, long after the invention of underwater sonar imaging by Paul Langevin at the beginning of the 20th century [1]. For this historical reason, the way in which we produce an image in medical ultrasound is intimately linked to the concept of echolocation in underwater acoustics. First, using single focused elements (A-mode), ultrasound devices were used to record backscattered echoes at depths along a focused beam line. During a short period in the 70s, ultrasonic images were then acquired by moving the focused transducer mechanically [2]. As a consequence, with the development of multiple element arrays and electronic focusing, line-per-line acquisition has become the core technology used in all ultrasound scanners [2]. In this way, medical ultrasound imaging is clearly a heritage of sonar.

However, the concept of using plane waves to insonify a very large field of view in a single transmission and then building an image from the resulting backscattered echoes differs from sonar. In fact, this technique is more similar to optical concepts, particularly optical holography, which was invented by Denis Gabor in 1948 [3]. Indeed, optical holography is a method that allows a light field, which is generally the product of a light source scattered off a complete object, to be recorded on a holographic plate based on interference with a plane reference field. Using

a nonlinear process, the interference of these waves transforms the phase information of the incident wave, which is necessary but unavailable, into experimentally available intensity information. The interference is later reconstructed when the original light field is no longer present, because of the absence of the original object. Illumination of the holographic plate by the complex conjugate of the plane reference wave allows for the generation of a complex conjugate of the incident wave (i.e., the hologram of the initial object) (Fig. 1).

In ultrasound, such a holographic approach does not require nonlinear effects because reversible transducers can be used to record both the phase and amplitude of ultrasonic wavefields. A holographic experiment can be performed thanks to the concept of time reversal ultrasound, which was proposed by M. Fink in the 1980s [4], [5]. Similar to optical holography, time reversal ultrasound involves transmission of a wide field-of-view wavefront into the medium, which is followed by recording of back-scattered echoes on an ultrasonic array. Time reversing of these echoes, which consists of re-emitting previously recorded echoes in a reversed chronology, builds a wavefield that refocuses optimally on the initial object during backpropagation. At the time of refocusing, the spatial distribution of the wavefield corresponds to the physical image of the object. Such time-reversed propagation can be used to either physically refocus on selected targets for destruction/aberration corrections in adaptive focusing [6] or to virtually recreate an image of the initial scattering object in the computer (Fig. 1). This second approach, corresponding to a numerical time reversal experiment, in which the time-reversed echoes are refocused on the initial object in a numerical model of the propagation medium (with a constant and homogeneous sound speed), was introduced in the 1980s independently of the time-reversal concepts. It is usually referred to as **digital parallel receive beamforming** in the literature.

Therefore, ultrafast ultrasound imaging utilizes concepts that come from optical holography and ultrasonic time reversal. Overall, this imaging technique consists of transmitting a wide field-of-view beam into the medium, recording the resulting backscattered echoes, and finally performing digital parallel beamforming (or time-reversal focusing) of the echoes to computationally build the final ultrasonic image from a single transmission.

Optical holograms are recorded using a single flash of light that illuminates a complete scene and is imprinted on a recording medium. Subsequently, a second illumination is utilized to recreate the phase conjugate of the initial interference. In contrast, ultrafast ultrasound insonifies the medium with a single plane wave, and the

Manuscript received October 1, 2013; accepted October 18, 2013. M. Tanter and M. Fink are co-founders and shareholders of Supersonic Imagine company.

The authors are with the Institut Langevin, École Supérieure de Physique et de Chimie Industrielles de la Ville de Paris (ESPCI), CNRS, INSERM, Paris, France (e-mail: mickael.tanter@espci.fr).

DOI <http://dx.doi.org/10.1109/TUFFC.2014.2882>

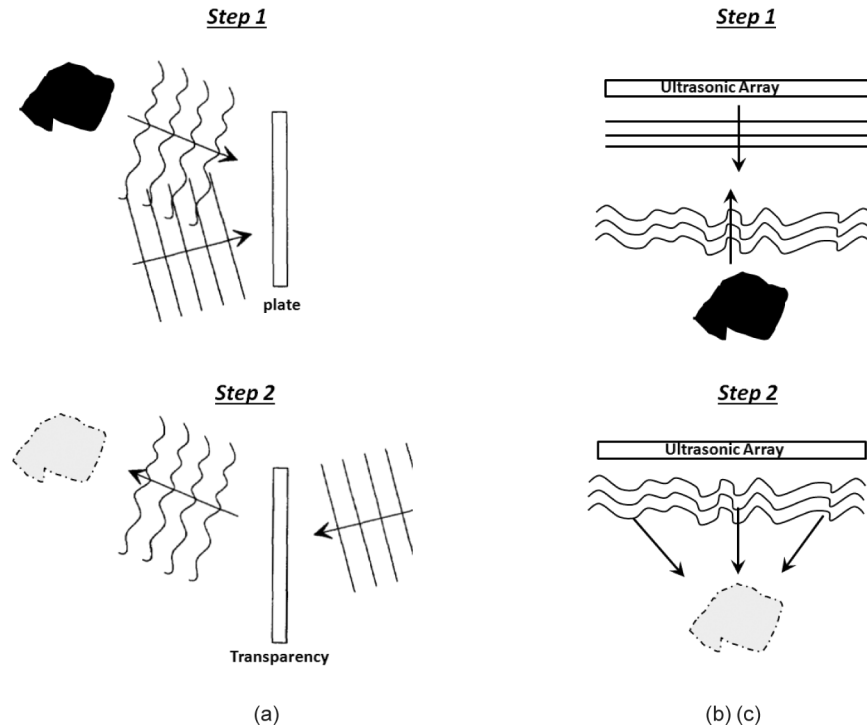


Fig. 1. Analogy between the two steps employed in (a) optical holography, (b) time reversal, and (c) ultrafast ultrasound imaging. (a) Optical holography: step 1, transmission of a wide-field light beam and recording of interference of the scattered and reference beams on the plate; step 2, phase conjugate generation of the incident beam is achieved by illuminating the plate with a reference beam. (b) Ultrasonic time reversal: step 1, transmission of a wide-field wavefront and recording of echoes on the array; step 2, transmission of the time-reversed echoes, whose propagation recreates the initial object shape. (c) Ultrafast ultrasound imaging: step 1, transmission of a wide-field wavefront and recording of backscattered echoes on the array; step 2, digital parallel beamforming of the echoes to recreate the initial object shape. One can observe that (a), (b), and (c) are extremely similar. The single and subtle difference between (b) and (c) stems from the fact that in step 2 of time reversal, waves physically refocus in the medium, whereas in step 2 of ultrafast ultrasound imaging, waves numerically refocus in a model medium (assumed homogeneous) as a result of digital parallel beamforming.

backscattered echoes are time reversed (wideband analog of phase conjugation) and numerically backpropagated to recreate the initial ultrasonic scene.

More than sixty years after their discovery, optical holograms are mainly used in art. However, this technology has the potential to be utilized for engineering next generation storage devices, because it displays more storage capacity than Blu-Ray platforms (i.e., the entire volume of the recording media can be exploited, instead of just the surface). In ultrasound, the development of ultrafast scanners based on plane-wave imaging and parallel beamforming processing have the potential to revolutionize medical ultrasound imaging; however, with time this technology could also be used for advancements in other fields.

II. THE PRECURSORS OF ULTRAFAST IMAGING

The concept of ultrafast echographic imaging was introduced more than thirty years ago. In 1977, Bruneel *et al.* first coined the ultrafast terminology in a seminal paper entitled "Ultrafast echotomographic system using optical processing of ultrasonic signals" [7]. However, because the technology in the 1970s was not sufficiently quick enough, they had to develop a smart system in which the informa-

tion was carried by an acoustic wave that was impressed on a light beam diffracted during the acousto-optic interaction. An optical system was then used to display a real image of the insonified object. Using this approach, they were able to develop an imaging system based on 20 transducers working at a very high frame rate (1000 fps). The visionary conclusion of their work was that "the fast motion picture capability makes our system very attractive with respect to others under development which use serial line-by-line processing." In 1979, this same research group moved from this acousto-optic system to the use of receiving electronics with analog parallel processing. In fact, Delannoy *et al.* demonstrated the power of such analog-based parallel processing approaches by developing an ultrasound system able to produce entire frames simultaneously from a single acoustic pulse [8]. Their scanner was capable of reaching a frame rate of 1000 images per second, with 70 lines per frame. Delannoy *et al.* intended to reach the physical limits of ultrafast imaging with their system, explaining that "a heart image, for instance, can be visualized in 200 μ s at an exploration depth of 15 cm, allowing rates up to 5000 images per second." Nevertheless, it took more than thirty years to finally demonstrate the use of such parameters over a large field of view in clinical cardiac configurations [9].

Years after the pioneering work of Bruneel and Delannoy, Shattuck *et al.* implemented a parallel processing approach for a phased-array sector scanner, which enabled the simultaneous acquisition of several B-mode lines from each transmitted acoustic burst [10]. This approach was named explososcan by the authors, and they validated the system *in vivo*. The first explososcan system was based on the single transmission of a slightly defocused ultrasonic beam and the parallel processing of four ultrasonic beams in the receive mode [10]. Also, implementation of the approach for volumetric imaging was later proposed [11]. Thus, the initial system increased the data acquisition rate four times [12]. After this first successful attempt to increase the frame rate, they envisioned that this method could be, at least conceptually, extended to the imaging of complete tomographic planes from echoes produced by a single transmitted pulse. However, for this, the pulse would need to fully illuminate the region of interest.

Parallel to the work of Delannoy, Fink proposed [13] a time-reversal approach to implement parallel processing using an analog time-reversal processor, which was made up of two ultrasonic arrays immersed in a fluid tank with an ultrasound speed identical to that of tissues. Later, in the early 1990s, Fink *et al.* developed a technology that made use of time reversal mirrors based on analog-to-digital converters [14]. This multi-channel system consisted of hundreds of fully independent analog transmit/receive boards, which were capable of driving transducer arrays with high versatility (both in transmit and receive modes). As a result of this technology, an important limitation to ultrafast imaging was overcome fifteen years after the time-reversal approach was proposed, when Fink's research group [15]–[17] demonstrated that the concept of plane-wave illuminations and massive parallel receive beamforming could lead to ultrafast frame rates that were higher than a thousand frames per second. Moreover, these frame rates were capable of capturing pertinent information on tissue motion. In those years, the primary goal for such ultrafast technology was to achieve real-time imaging of the transient propagation of shear mechanical waves in human tissues for the assessment of local viscoelastic properties, a technique initially dubbed transient elastography. This ultrafast approach led to the first *in vivo* clinical investigation of ultrafast imaging for breast cancer diagnosis [18].

Another approach for reaching high frame rates was reported by Lu and Greenleaf in the 1990s and was based on the use of nondiffracting beams [19]–[22]. Following this pioneering work, Lu *et al.* developed a theory in which a pulsed plane wave could be used in transmission, with limited-diffraction array beam weighting applied during reception, to produce a spatial Fourier transform of the object function for 3-D image reconstruction. Later, he proposed the use of spatial compounding with different limited-diffraction beams added in a coherent way to enhance resolution, or in an incoherent way to reduce speckle [23], [24].

In 2002, another significant advancement was made in plane-wave imaging technology when Tanter *et al.* introduced plane-wave compounding for vector tissue motion imaging in transient elastography [16]. This successive transmission of tilted plane waves with different angles was introduced to enable ultrafast vector tissue Doppler imaging. Notably, the incoherent averaging of vector tissue motion estimates, which were obtained from the different plane-wave transmissions, was essential for insuring the quality of transverse motion estimates. This concept of incoherent plane-wave compounding was also applied to improve ultrasonic imaging of temperature changes [25].

Unfortunately, although plane-wave imaging at very high frame rates (>1000 frames per second) for transient elastography gave very good results in moderately heterogeneous speckle medium (e.g., breast) [18], [26], its use was limited in complex and heterogeneous speckle media (e.g., muscle). In an attempt to overcome this limitation, coherent synthetic summation of ultrasonic images acquired with different plane waves at tilted angles was introduced to virtually rebuild the transmit focusing process for conventional imaging [27]. Relying on dynamic focusing in both transmit and receive modes, this coherent beamforming process allowed for better image quality in plane-wave compounding compared with conventional ultrasound without compromising the ultrafast frame rate (Fig. 2). This is due to the fact that coherent summation of tilted plane waves re-synthesizes a dynamic transmit focus at each depth. This idea of virtual dynamic transmit focusing was introduced by Cooley and Robinson in 1994 [28], as part of a framework for synthetic focus imaging. Although Cooley and Robinson briefly described the implications of a small number of transmissions, Montaldo *et al.* experimentally applied this concept of coherent summation of virtual dynamic transmit focusing to plane-wave transmissions, which ultimately resulted in coherent plane-wave compounding [27].

Parallel to the work on plane-wave beamforming for very high frame rate imaging, the research groups of Jensen [29]–[34] and Lockwood [35], [36] made important contributions in the field of non-conventional beamforming with synthetic aperture imaging. Initially based on single element transmissions and synthetic recombination of backscattered echoes, this synthetic aperture imaging approach was not applied to ultrafast imaging because the number of transmit events was similar to that of conventional line-per-line focusing. However, this technology was used to improve B-mode and Doppler imaging. To increase the frame rate of synthetic aperture imaging, the use of sparse synthetic transmit aperture (i.e., sparse distribution of single transmit elements of the array) was simulated for real-time 3-D imaging [35], [36]. Sparse synthetic aperture imaging suffered from low SNR because the transmission was limited to single elements. For this reason, based on a suggestion by Karaman *et al.* [37], Lockwood *et al.* simulated sub-apertures made of several elements, which generated a diverging wave that cor-

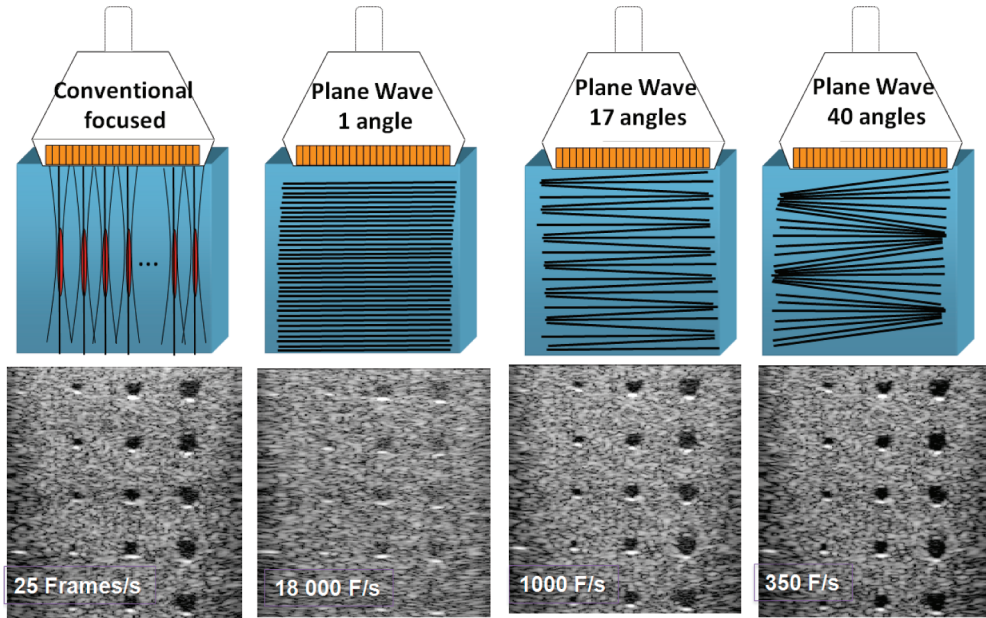


Fig. 2. Conventional focused and ultrafast ultrasound imaging sequences for a typical medical imaging setup (4-cm deep region of interest): (a) conventional focused imaging (128 focused beams and 4 focal depths leading to ~ 25 fps), (b) plane-wave imaging (~ 18000 fps), (c) plane-wave compounding with 17 angles (~ 1000 fps), and (d) plane-wave compounding with 40 angles (~ 350 fps). 

responded to a virtual ultrasound source located behind the array [35]. In addition, Nikolov *et al.* studied virtual ultrasound sources located behind the array in synthetic aperture imaging [38]. Each transmission corresponded to a subaperture that was composed of elements firing at different times to generate a diverging wave. They used multiple transmit elements (typically ~ 10) and only a few emissions (4 to 8) to increase the frame rate [38], which resulted in a compromise between ultrafast imaging (full array aperture) and synthetic aperture imaging (single element aperture). Similarly, bridging the two concepts of ultrafast plane-wave imaging and synthetic aperture imaging, McLaughlin and colleagues proposed a broad-beam scanning approach [39], [40] which was based on transmit beams that focused on regions (called zones). These zones were much broader than conventional line-per-line acquisitions. For 3-D fast imaging, Hossack *et al.* recently proposed 2-D array beamforming, which is based on separable line array beamforming operations that allow for increased frame rate and energy efficiency in hand-held devices [41].

Today, after more than 25 years of intensive investigation, this technology has begun to move out of academic labs and become incorporated into commercially available clinical products. Indeed, ultrafast plane-wave imaging has been employed in the first ultrafast clinical scanner, the Aixplorer system, since 2008 (Supersonic Imagine, Aix en Provence, France). Also, the broad-beam technology is being used in the clinical Zonare Z.one scanner (Zonare, Mountain View, CA). Finally, other devices, such as the Verasonics platform (Verasonics, Redmond, WA), have been commercialized for use in academic research labs.

III. THE CONCEPT OF PLANE-WAVE IMAGING AND PLANE-WAVE COMPOUNDING

Plane-wave imaging represents a genuine change in the medical ultrasound paradigm. Instead of transmitting focused beams, which scan the whole region of interest line-per-line, ultrafast imaging is obtained by transmitting plane (or unfocused) waves which scan in a single transmit event over the whole region of interest. This method typically increases the frame rate more than 100-fold. However, in transient elastography, this huge increase in frame rate was initially achieved through a compromise in image quality [15]. This degradation of quality mainly affected the image contrast rather than the resolution. Because the goal of this imaging modality was to track tissue displacement induced by shear wave propagation, this loss in resolution was an acceptable price compared with the advantages provided by ultrafast frame rates [16]–[18]. Several articles have thoroughly discussed the differences in contrast and resolution obtained when using conventional plane-wave imaging, and plane-wave compounding [27], [42], [43].

Coherent plane-wave compounding has many advantages because it provides an image of a full region of interest for each ultrasonic transmission using all array elements. First, the transmission of a plane wave on the whole array aperture generates a much higher amplitude signal than synthetic aperture imaging. Second, the insoufflement of the whole region of interest for each transmitted plane wave permits the construction of high-quality ultrasonic images with a limited number of compounded plane waves because the acquisition is performed within a

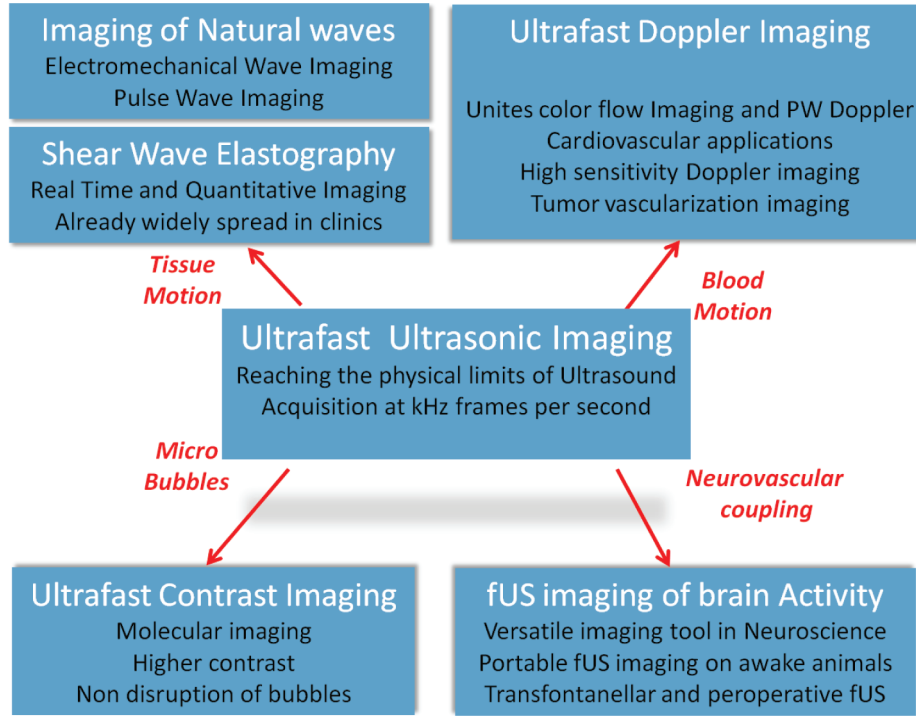


Fig. 3. Some emerging and future applications of ultrafast ultrasound imaging.

very short period of time (hundreds of microseconds), enabling measurement of tissue motion, blood motion, and contrast agent dynamics with frame rates in the kilohertz range. Indeed, this has paved the way for groundbreaking applications of this technology (Fig. 3). For example, imaging of transient dynamics of raw ultrasonic data in the kilohertz range gives access to mechanical vibrations induced by the propagation of operator-induced shear waves (Section IV) or intrinsic mechanical or electromechanical waves (Section V). When imaging contrast agents, it provides improved contrast imaging and information about the local medium properties (Section VI). When imaging blood motion, this technique can provide a full 2-D characterization of complex blood flow by merging currently incompatible modes [i.e., color flow imaging and pulsed wave (PW) Doppler modes] (Section VII). It also allows detection of slow flow in very small vessels, which has paved the way to ultrasonic imaging of brain activity via functional ultrasound (fUltrasound) (Section VIII). Finally, ultrafast ultrasound technology has begun to be used in other research fields beyond medical ultrasound (Section IX).

It is important to keep in mind that the ultrafast terminology describes any acquisition sequence enabling 2-D or 3-D imaging over a large field of view at very high frame rates, typically in the kilohertz range (i.e., the combination of wide-field transmissions and parallel receive beamforming). In the last two decades, ultrafast imaging has never been done in real time because the processing of such ultrafast imaging sequences has always been slower than the acquisition rate. Nevertheless, this technology

has shown many valuable clinical applications. Moreover, as seen in Fig. 4, we are very close to achieving real-time processing in ultrafast imaging.

Today, the computational power produced by graphical processing unit (GPU)-based platforms (e.g., Nvidia GeForce technology [\sim 1500 GFlops in 2013]; Nvidia Corp., Santa Clara, CA) and high-speed buses (e.g., PCI Xpress [4 GB/s]) is typically capable of transferring and computing the beamforming of 100 frames from 100 successive wide field-of-view RF data transmissions at 10 kHz. Strikingly, this information is acquired using a 128-element array on a GPU board in less than 0.25 s (for a typical 5-cm depth image at 60 MHz). Indeed, this transfer and computation time is already sufficient to produce a complete movie of several shear waves propagating through large organs. Thus, this plane-wave imaging is valuable for many clinical applications, including shear wave elastography [26] (for which the data acquisition and building of quantitative images of elasticity typically requires 0.25 s). It also permits a shorter time for post-processing (2 to 4 s) to fully characterize (pixel-per-pixel PW Doppler) complex blood flows over a complete cardiac cycle using an ultrafast frame rate (>1000 Hz) and to visualize a wide 2-D field of view. PCI Xpress transfer rates and GPU computational power also allow conventional grayscale ultrasonic imaging based on line-per-line acquisitions in real time, which has led to the first full software-based clinical systems that perform image construction with software instead of hardware (e.g., Aixplorer, Supersonic Imagine). Nevertheless, this current technology is insufficient for performing grayscale imaging in real time (with

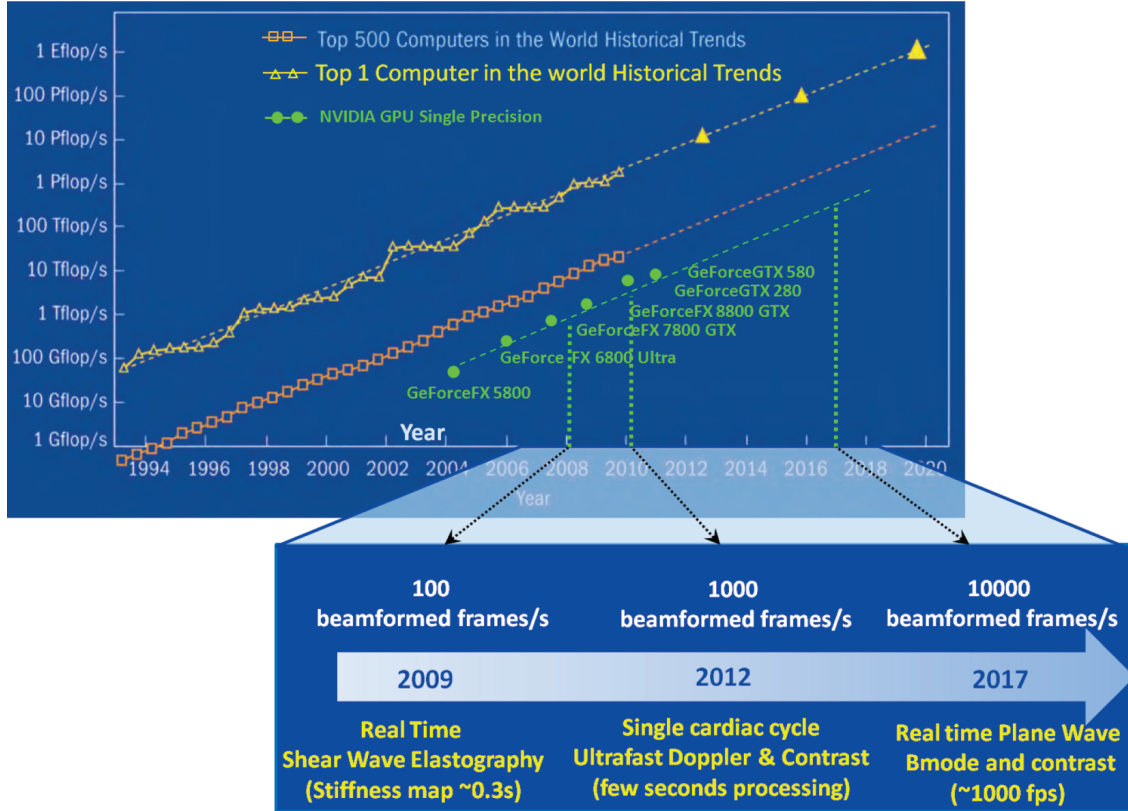


Fig. 4. Moore's law (adapted from [44]) applied to the world's top computer, the world's top 500 computers, and public GPU technology (e.g., NVidia GeForce series). Note that the power law is similar for supercomputers and commonly available GPU technology. For example, using the Nvidia GPU GeForce series, the implications of an increased number of operations per second is shown for medical ultrasound and emerging ultrafast imaging modalities (using a 128-element array). In 2009, at 1.5 Tflop/s was already possible to perform shear wave elastography based on typical 10-ms periods of ultrafast imaging (several times per second). In 2012, at 10 Tflops, a full 1-s cardiac cycle acquired at 10 kHz could be post-processed in 2 or 3 s and displayed on the scanner. In 2017, at 50 Tflops, it should be possible to perform real-time B-mode imaging at kilohertz frame rates.

typical frame rates of 25 fps) based on ultrafast compounded plane-wave transmissions instead of line-per-line acquisitions. Furthermore, based on the evolution of computational power in the last decade [44], the extrapolation of Moore's law for commonly available GPU technology (e.g., NVIDIA GPU GeForce Series) predicts that the potential use of compounded plane-wave transmissions instead of line-per-line acquisitions for optimal real-time B-mode imaging could occur around year 2017, because it will require approximately 50 Tflop/s (Fig. 4). Thus, in the near future, it is likely that high-quality B-mode imaging will be obtained through dynamic focusing in both transmit and receive modes.

IV. ULTRAFAST IMAGING OF SHEAR WAVES

The first clinical application of ultrafast imaging was introduced in the field of elasticity imaging with the goal of solving the limitations of static elastography (nonquantitative imaging) and dynamic elastography (monochromatic vibrations inducing complex 3-D vibrations patterns). For the latter, the objective was to track in real

time the shear waves induced by a transient vibration from the surface of the body, a method called transient elastography [16]–[18]. Because shear waves typically propagate at speeds of 1 to 10 m·s⁻¹, ultrasonic frame rates higher than 1000 fps were mandatory for real-time tracking of these transient mechanical vibrations. Ultrafast imaging provided a 2-D transient movie of shear wave propagation with the following features: 1) the results are uncorrupted by longitudinal mechanical waves, as is the case for magnetic resonance (MR) elastography [45], [46] and sonoelasticity [47]; 2) breathing and/or cardiac motion artifacts can be easily filtered out of the shear wave propagation because they occur on a slower time scale; and 3) the high spatial and temporal sampling rates can benefit local estimations of quantitative shear wave speed and stiffness.

Although the concept of transient elastography for elasticity imaging has shown promising preliminary clinical results in breast cancer studies [18], its applicability in daily clinical practice has been limited by the use of heavy external mechanical vibrators. In parallel to this work, several other groups evaluated the possibility of using the acoustic radiation force impulse (ARFI) induced

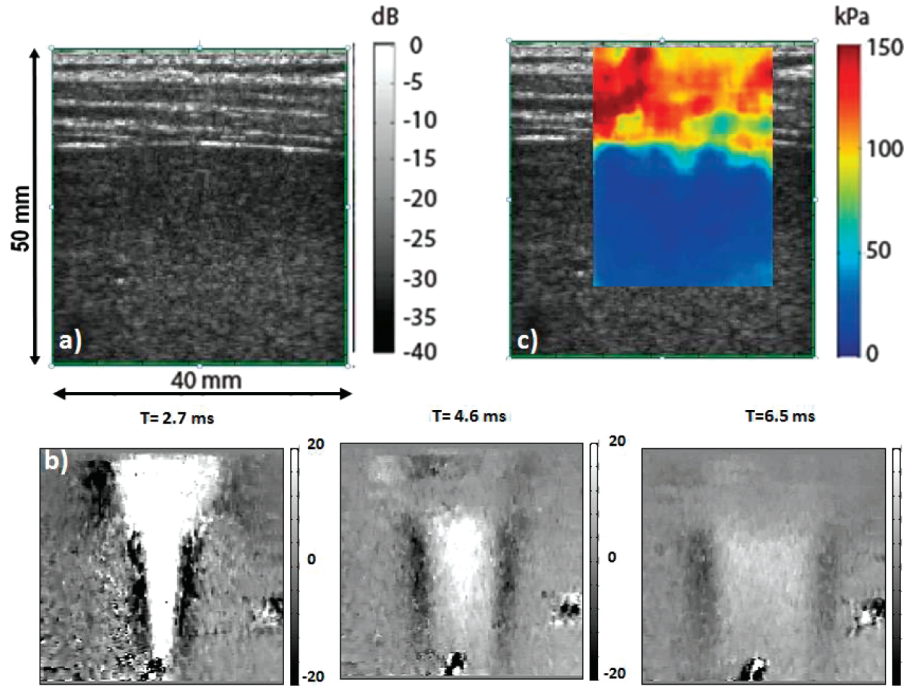


Fig. 5. Ultrafast plane-wave imaging of shear waves propagating in the liver of a healthy volunteer: (a) ultrasonic B-mode image, (b) snapshots of local tissue displacement (in micrometers) at 2.7, 4.6, and 6.5 ms following shear wave generation, and (c) the resulting quantitative tissue stiffness map (Young's modulus in kilopascals ranging from 0 to 150 kPa). 

by the ultrasonic probe itself as a remote and localized palpation [48], [49]. This involved measurement of local tissue displacement using conventional ultrasonic imaging (line-by-line focused beams). The tissue displacement was estimated only at the push location, and the radiation force push had to be repeated at many different locations to provide a 2-D qualitative map of tissue stiffness. In the last decade, this technique, called ARFI imaging, has been applied to several *in vivo* clinical diagnostic procedures [50].

In 2004, Bercoff *et al.* proposed to combine the advantage of transient elastography (ultrafast plane-wave imaging of shear waves) with remote palpation induced by the acoustic radiation force [51]. This technique called supersonic shear wave imaging (SSI) solved the problem of using heavy surface vibrators, while taking advantage of the speed of ultrafast imaging. Fig. 5 shows an example of SSI imaging of a liver from a healthy individual. The ultrasonic B-mode image clearly delineates a bilayered image that corresponds to the intercostal muscular space and the liver [Fig. 5(a)]. The displacements induced by the acoustic radiation force in the organ are imaged at an ultrafast frame rate [Fig. 5(b)]. Three snapshots of local tissue displacement (in micrometers) at 2.7, 4.6, and 6.5 ms after shear wave generation in the middle of the imaged plane are displayed [Fig. 5(b)]. Estimation of the local shear wave speed from this ultrafast movie allows generation of a quantitative map of tissue stiffness (Young's modulus E in kilopascals) [Fig. 5(c)]. The greater stiffness of the intercostal muscle compared with the soft and homogeneous liver tissue can be clearly visualized.

The word supersonic is used to allude to a particular way of generating cylindrical shear waves by moving the radiation force push location down into organs at a supersonic speed (i.e., the push displacement speed is higher than the shear waves that it generates, leading to a Mach cone) [52]. This geometry limits the diffraction of the shear wave in the imaging plane, thus inducing propagation over larger distances compared with single push generation. However, the supersonic cone is a secondary feature of the SSI method, which combines ultrafast imaging and acoustic radiation force palpation.

Recently, a refinement of the ARFI imaging technique [called ARFI shear wave speed (ARFI SWS)] has been proposed to track shear waves as in SSI [53]. Using slightly defocused beams in the transmit mode (also known as fat beams) and a four-line parallel beamformer in the receive mode, a movie comparable to the one with the SSI approach can be obtained (typically repeating the radiation force 20 times at the same location and recombining the respective movies acquired along the four lines). Unlike ultrafast imaging of shear waves, the potential motion artifacts that occur in ARFI SWS during zone-by-zone acquisition of the complete shear wave propagation movie require the use of refined motion-correction post-processing approaches [54]. Moreover, because of acoustic safety issues, repetition of radiation force pushes at the same location makes it impossible to obtain real-time quantitative stiffness imaging. This comparison emphasizes the advantages of ultrafast imaging in elastography, because it currently represents the only way to provide a 2-D real-time (>2 fps), quantitative image of tissue stiffness [55].

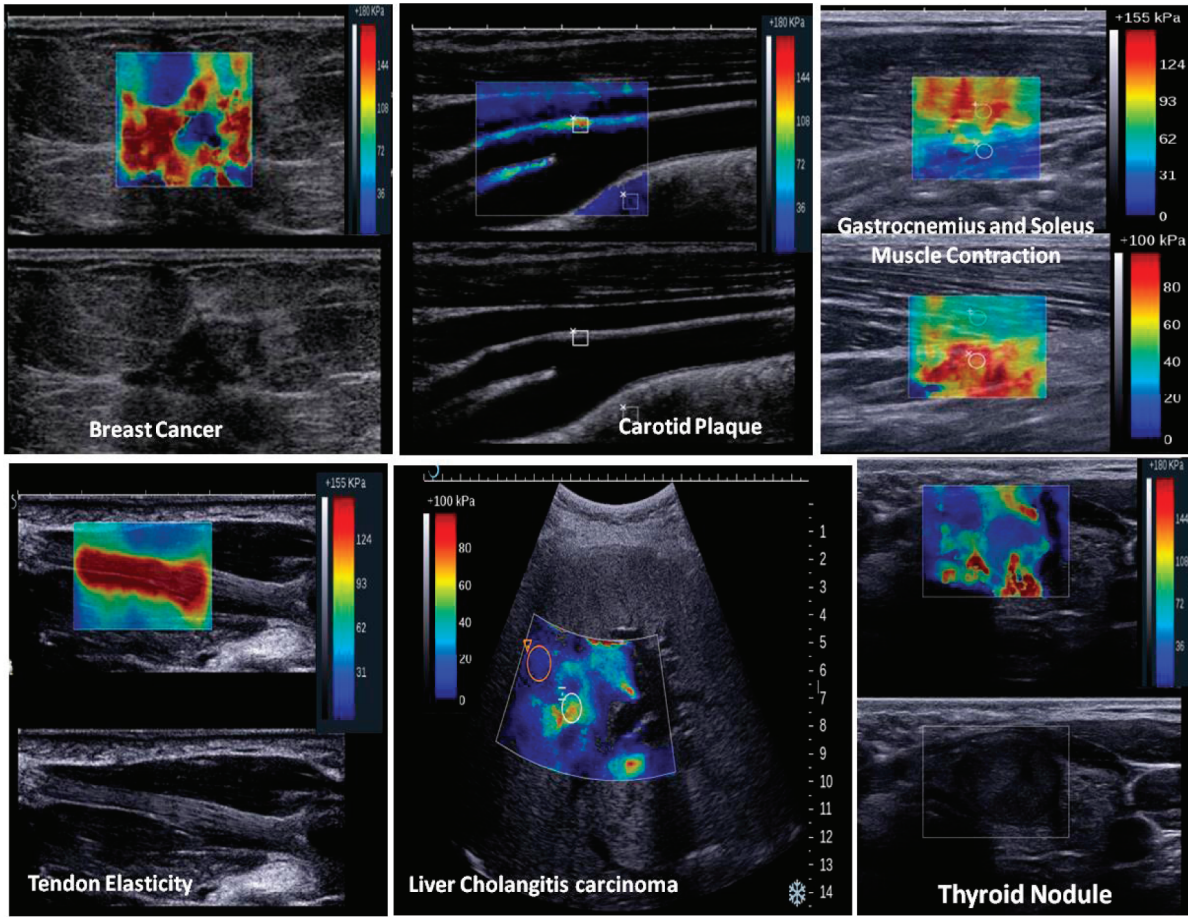


Fig. 6. Clinical examples of shear wave elastography based on the supersonic shear wave imaging (SSI) method (courtesy of Supersonic Imagine, France).

In fact, this technique has already paved the way to 3-D quantitative elasticity mapping over reasonable acquisition times (i.e., over several seconds).

In the last five years, a large number of clinical validations of the SSI method have been performed in various fields, including breast cancer diagnosis [26], [56], [57], liver fibrosis staging [58]–[60], musculoskeletal imaging [61]–[63], arterial rigidity imaging [64], cardiac elasticity imaging [65], [66], and ophthalmology [67] (Fig. 6). Beyond clinical diagnosis, it also offers a promising approach for the monitoring of RF ablation, high-intensity focused ultrasound [68], [69], or histotripsy treatments [70] (the therapeutic beam strongly affects the local mechanical properties) [71]. Other similar approaches based on ultrafast imaging are also currently under investigation [72]. Finally, the development of clinical ultrasound scanners based on ultrafast plane-wave imaging (Aixplorer, Supersonic Imagine) which feature full software-based beam-forming are permitting this basic physics concept to be utilized in the clinic.

V. ULTRAFAST IMAGING OF INTRINSIC WAVES

Beyond the shear waves induced by the ultrasonic radiation force, ultrafast frame rates can also be used to track

natural or *intrinsic* vibrations in organs. As long as we are alive, our body constantly exhibits transient vibrations, which propagate through most organs. These vibrations mostly spread as shear waves, and are created by several physiological processes, including mechanical contraction of our heart, vibrations induced by our vocal cords during speech, and propagation of action potentials in our muscles. In addition, the movement of blood through large arteries applies a transient mechanical stress on the surrounding organs, particularly in confined organs such as the brain or kidney.

H. Kanai and colleagues pioneered ultrasonic imaging of these intrinsic mechanical waves in the field of cardiovascular imaging [73]–[75]. Although they did not have access to an ultrafast scanner in 2000, they were able to image the transient propagation of mechanical waves in the heart by repeating the experiment over several cardiac cycles and reconstructing an ultrafast movie of cardiac tissue motion. In 2005, Pernot and Konogafou used the same stroboscopic approach to track the propagation of electro-mechanical waves in the myocardium of rodents [76]–[78]. In 2006, Deffieux *et al.* made the first ultrafast plane-wave acquisitions of electromechanical waves propagating in human biceps following electrical stimulation [79]. To illustrate the potential of ultrafast imaging, they studied both

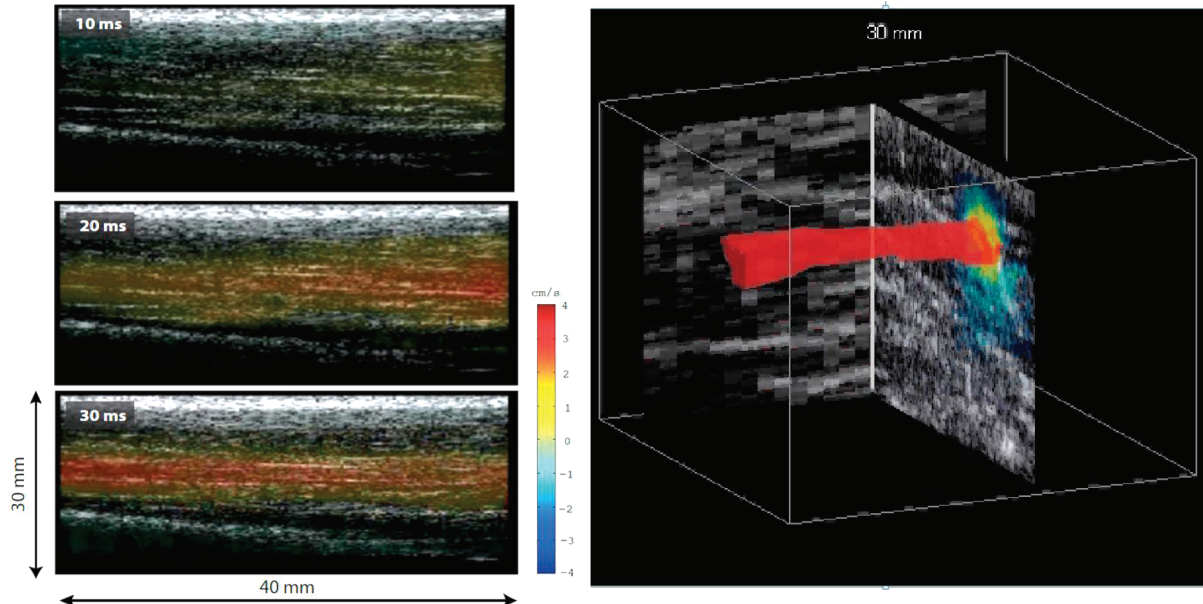


Fig. 7. The first ultrafast imaging of fiber contraction induced by the propagation of an action potential during transient electrical stimulation: (a) *in vivo* longitudinal acquisitions (along the fibers) of a human biceps brachii, (b) the same experiment performed in the transverse plane (perpendicular to fibers), and (c) repeating the experiments in several planes allows identification of the high mechanical energy regions (red contours), corresponding to the recruited fiber bundles (from ref [61]).

the 2-D and 3-D spatial distribution of *in vivo* muscle fiber recruitment as a function of the electrical stimulus (Fig. 7). Subsequently, the first ultrafast imaging experiments of electromechanical waves in a single heartbeat of cardiac muscle were performed by Couade *et al.* in sheep [9].

In parallel to the aforementioned studies, very important work was performed by the research groups of E. Konofagou [80]–[83] and H. Kanai [84] on the stroboscopic imaging of cardiac electromechanical waves using electrocardiogram (ECG)-gated conventional ultrasound imaging. Furthermore, in 2011, Provost *et al.* demonstrated that the speed of electromechanical waves imaged by ultrasound is strongly correlated to propagating electric waves in a dog's heart [83]. In 2012, Provost *et al.* also performed single-heartbeat electromechanical wave imaging using temporally unequispaced acquisition sequences [85], performing the first clinical evaluation of electromechanical wave imaging (EWI) in patients [86].

In addition, wave propagation through the vasculature of our organs is of particular interest for medical diagnoses. This mechanical wave, known as a *pulse wave*, has been intensely studied in the field of biomechanics [87] and has been used for years to diagnose cardiovascular diseases and to evaluate cardiovascular risk. Notably, this physiological wave is initiated during systolic peak pressure, which corresponds to the ejection of blood through the aorta. Because the arterial wall is elastic, this local overpressure results in an increase of the aortic radius, which propagates along the aorta and the arterial tree. Through analysis of the properties of this wave, such as its velocity and its shape, information can be retrieved regarding arterial stiffness. Today, most existing techniques for estimating arterial stiffness are based on analysis of

the pulse wave traveling through the artery. The most widely used clinical technique allows the estimation of the pulse wave velocity (PWV) at very distant sites and can be performed by measuring the coupled pressure wave, using two or more pressure sensors attached to the skin [88]. Although this method is robust and gives an average estimate of the PWV, Young's modulus is not accurately estimated by this procedure because of bias in the estimation of the distance between the two measurement sites. Thus, to obtain a local estimate of the PWV, ultrasound and magnetic resonance imaging (MRI) have been used for measuring radial displacements caused by the pulse wave propagation. However, these attempts have been limited by the fact that the transit time of the pulse wave through the imaged region is small compared with that of conventional imaging frame rates of both modalities. Recently, several studies highlighted the potential value of ultrafast imaging for local measurement of arterial pulse waves [89]–[92]. Again, ultrafast frame rates are a critical step for achieving real-time tracking of pulse wave propagation in the 2-D imaging plane within a single cardiac cycle.

VI. ULTRAFAST IMAGING OF CONTRAST AGENTS

In ultrasonic contrast imaging, the injection of microbubbles is currently used to enhance the contrast from blood, thus improving the visualization of vessels that are undetectable during conventional Doppler imaging (e.g., the coronary chamber or myocardium vascular network) [93]. Contrast imaging can also be used to monitor blood perfusion into tissues for tumor imaging (e.g., liver ap-

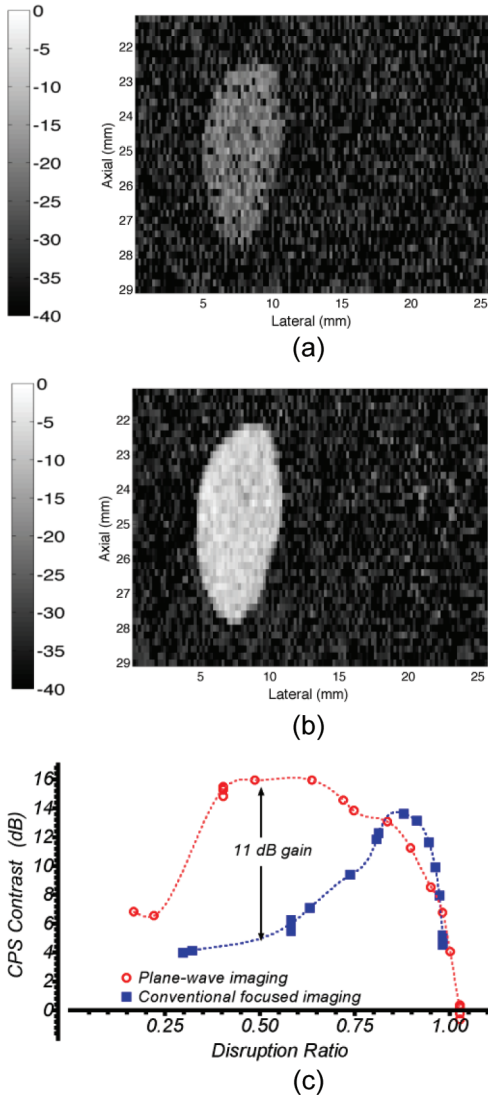


Fig. 8. Image obtained with (a) conventional contrast imaging and (b) plane-wave imaging for a similar disruption ratio of microbubbles (gray-scale in decibels). (c) Contrast-to-tissue ratio using the contrast-pulse sequence (CPS) method with plane-wave and conventional line-per-line imaging. To preserve 50% of the bubbles after 100 images, peak-negative pressure had to be reduced for conventional focused imaging, and only 5 dB in contrast is observed with respect to the tissue-phantom. At the same disruption ratio, plane-wave imaging attains 16 dB in contrast-to-tissue ratio (adapted from [107]).

plications) [94]. Furthermore, by functionalizing microbubbles with antibodies or short-peptides, it is possible to drastically enhance their affinity for thrombi, arteriosclerotic plaque [95], and neo-vasculature [96] in specific biological targets to facilitate molecular imaging.

In this regard, the concept of ultrafast imaging is of interest based on the following features:

A. Ultrafast Imaging of Bubble Disruption

Monitoring the scattering properties of ultrasound contrast agents following disruption can provide useful information on their environment as well as relevant physiologic data. Such dissolution of post-disruption microbubbles

has already been studied with single-element ultrasound transducers [97], [98]. However, in clinical situations, conventional ultrasound cannot be used to track dissolving and moving microbubbles on millisecond time scales because of its insufficient frame rate. However, if ultrafast imaging and disruption sequences are alternated, then it becomes possible to track and image transient dissolution of contrast agents within a few milliseconds, as demonstrated by Couture *et al.* in 2009 [99]. In this case, the dissolution imaging sequence consists of subtracting successive ultrafast compound images. These dissolution imaging sequences highlight a peak in backscattering intensity that occurs just after the disruption pulse. Notably, this form of enhancement can increase the contrast from microbubbles during disruption-reperfusion imaging. Moreover, tracking the dissolution can help to distinguish microbubbles near a wall or those bound to a surface from the free-flowing agents. Indeed, while peak enhancement appears in the ultrafast images of freely moving bubbles within the first milliseconds following disruption, this phenomenon does not occur for surface-bound bubbles. Indeed, Couture *et al.* reported 2-D mapping of peak enhancement within the first 4 ms after disruption to distinguish bound and unbound bubbles. Such high temporal resolution could lead to new contrast imaging modalities, which could be used to assess the attachment of microbubbles to diseased cells or changes in arterial hydrostatic pressure [100]. In addition, ultrafast dissolution imaging can be utilized for monitoring remote drug delivery or tattooing using double nano-emulsion droplets activated with focused ultrasonic beams [101], [102]. Finally, ultrafast differential imaging is also key for *in vivo* estimation of cavitation threshold [103] or to actively image cavitation events [104]. Finally, Tanter and colleagues showed recently that ultrafast differential imaging could lead to ultrasonic microscopy by localizing contrast agents deep in organs. Such sono-activated ultrasound localization microscopy (SAULM) is the ultrasonic analog of fluorescence photoactivated light microscopy (FPALM) in optics [105].

B. Ultrafast Contrast Imaging

A major limitation in contrast imaging is that contrast agents can be disrupted by acoustic waves at fairly low pressures [106]. Unfortunately, these pressure levels are often required to induce the nonlinear behavior appropriate for their distinction from tissues. Thus, in conventional contrast imaging, the line-per-line sequence with focused pulses can destroy a large fraction of the microbubbles that are being tracked. Because of this sensitivity of microbubbles, sonographers generally must reduce the acoustic pressure and the frame-repetition frequency to a minimum (down to 1 image per second) to preserve the contrast agents. This trade-off dramatically reduces the amount of information available in perfusion and molecular imaging with ultrasound.

An interesting feature of microbubble imaging is that the disruption of contrast agents is mainly sensitive to

peak negative pressure, and to a lesser extent, the total acoustic energy. Thus, for sensing a desired location with a similar acoustic intensity, corresponding to a pixel in the image, the coherent summation of plane-wave compound imaging makes use of a large number of pulses at low acoustic amplitude. This is in contrast to conventional imaging, which uses one pulse at high peak pressure. In fact, our group demonstrated this concept of *ultrafast contrast imaging* by designing nonlinear pulse sequences for plane-wave imaging [107] (Fig. 8).

Notably, these plane-wave nonlinear sequences drastically reduce bubble disruption and improve the monitoring of their uptake during molecular imaging with ultrasound. For example, Couture *et al.* applied this sequence to the imaging of functionalized contrast agents targeting the overexpression of glycolipid Gb3 in tumor neovasculation [108]. The microbubbles were functionalized using a natural Gb3 ligand, the B-subunit of the Shiga toxin (STxB), and *in vivo* experiments performed on mice xenografted with human breast tumors demonstrated very specific tumor accumulation of STxB-labeled microbubbles (as compared with control microbubbles). Because ultrafast contrast imaging can be used for agents that display reduced disruption rates, it could represent a key modality in molecular ultrasound.

VII. ULTRAFAST DOPPLER IMAGING OF BLOOD FLOW

The ability of ultrasound to track blood flow dynamics within a single cardiac cycle represents a key feature of this medical imaging modality. Today, Doppler-based tools are mandatory on every medical ultrasound device, especially within the framework of cardiovascular and cancer diagnostic applications. Because of the intrinsic limitations of conventional imaging, two separate Doppler modes have emerged for use on clinical ultrasound devices in the last 30 years. One mode is based on the spectral analysis of the Doppler signal [i.e., the continuous wave (CW) or PW Doppler mode] with respect to the excitation signal, whereas the other is utilized for color-coded flow velocity imaging [109], [110].

Spectral analysis Doppler (PW Doppler) offers excellent temporal resolution and provides in-depth quantification of flow characteristics by means of measuring quantities, such as the peak flow velocity as a function of time, mean flow velocity as a function of time, resistance, and pulsatility indices within the cardiac cycle (i.e., the spectral broadening index) [109]. Spectral Doppler analysis requires continuous acquisitions or very high sampling rates (several thousand hertz). For this reason, flow quantification is typically available only at a single location (sample volume) or multiple locations along the same line (multi-gating) [111].

Color flow imaging (CFI) overcomes the limited spatial extent of spectral analyses by reducing the observation time at any given location and by spreading the line-per-line firings of the ultrasound over a 2-D region of interest.

However, this locally reduced observation time sacrifices the quantitative capabilities of CFI. Ultimately, the information obtained relates to the mean flow velocity and/or the estimated Doppler power over an extended area. Those modes are displayed in real time at frame rates that are usually quite low (approximately a few hertz).

These two separate modes, which have been implemented on all commercial devices for more than thirty years, result from the incompatible time resolution and spatial extent issues of line-per-line acquisitions. The major limitations of Doppler modes stem from the fact that physicians ideally require simultaneous real-time display of B-mode (grayscale) and PW-mode (duplex mode), and in some cases three modes (i.e., B, color, and PW modes; known as triplex mode). Duplex and triplex simultaneous modes have become standard on ultrasound systems, but suffer from limited frame rates in deep organs (e.g., liver or heart). Duplex and triplex modes represent major technical challenges, because they require complex sequencing, high-energy ultrasound transmission, and high processing power. Therefore, severe tradeoffs on imaging mode quality and/or frame rates are necessary.

Ultrafast imaging using unfocused transmissions offers a technologically disruptive solution to the problem of imaging and quantification for blood flow characterization. In fact, Bercoff *et al.* recently demonstrated that ultrafast Doppler based on plane-wave imaging could disrupt current incompatibilities that exist between imaging and quantification [112]. The ultrafast Doppler mode has now been implemented on a commercially available clinical scanner (Aixplorer, Supersonic Imagine). Indeed, plane-wave transmissions give access to high-precision characterization of complex vascular and cardiac flows because all pixels of the 2-D ultrasonic image rely simultaneously on a very high frame rate and a large number of temporal samples (i.e., long observation times). One major advantage of ultrafast Doppler for use in routine vascular imaging lies in the fact that all blood flow dynamics can be acquired during a limited number of cardiac cycles (typically one to three), and all PW Doppler pixel data for the whole image can be retrieved from the ultrafast sequence.

Finally, vector motion imaging based on plane-wave transmissions, which was initially proposed for monitoring tissue motion in shear wave elastography [16], was demonstrated to be valuable for vector-flow high frame rate imaging by J. Jensen's research group in 2008 [32] using their RASMUS research platform. Notably, investigations into the use of this technology for such applications have recently led to impressive *in vivo* results [113].

The use of ultrafast imaging during Doppler examinations permits the following:

- 1) adjustable positioning of the PW Doppler window (retrospectively) without requiring the probe to remain in the same imaging plane for a prolonged period of time;
- 2) several independent PW Doppler windows can be added, corresponding to simultaneous acquisitions

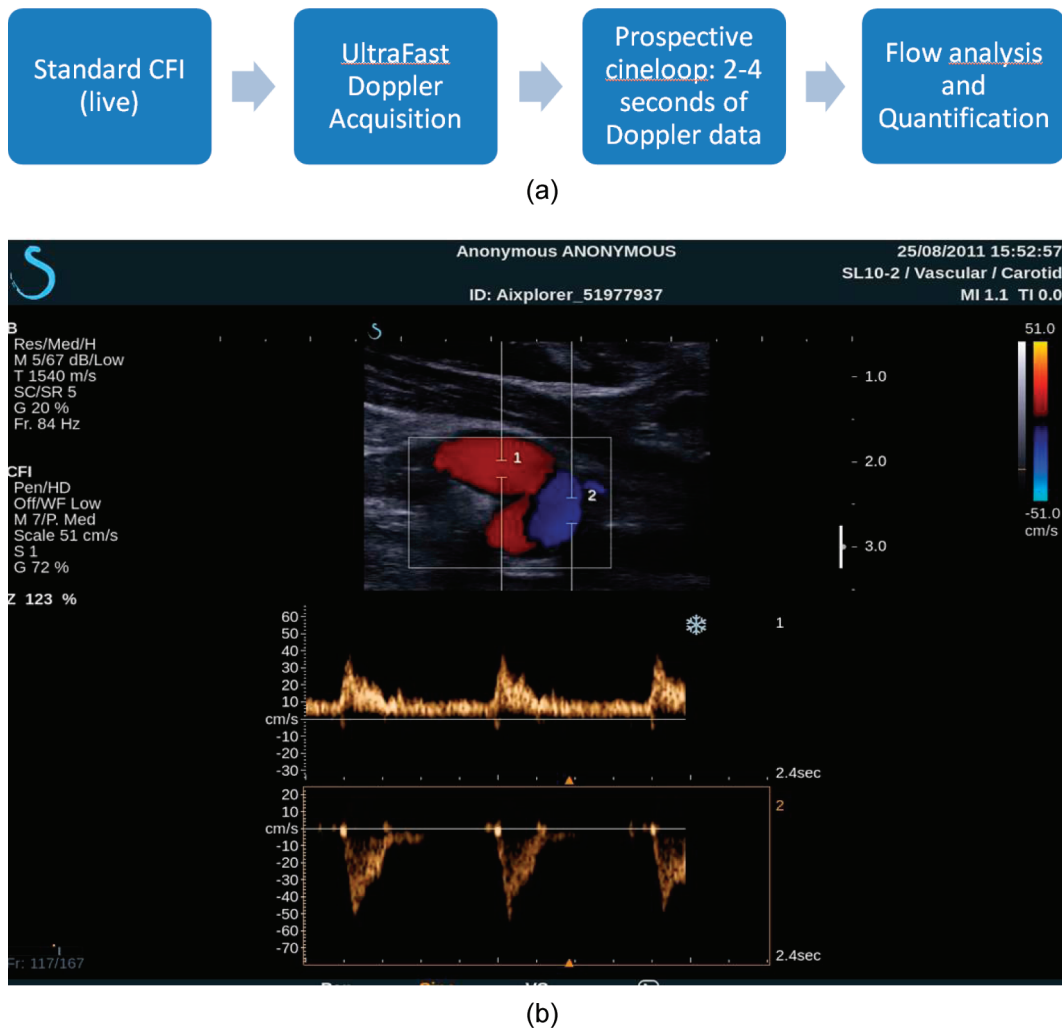


Fig. 9. Ultrafast Doppler imaging: (a) ultrafast Doppler protocol, (b) example of blood flow quantification obtained from ultrafast Doppler acquisitions (two simultaneous PW Doppler cursors can be placed at desired locations in different arteries; image courtesy of Supersonic Imagine). 

- at different locations and allowing comparison of blood flow at different locations without requiring several successive conventional PW Doppler exams;
- 3) blood flow dynamics within the same cardiac cycles can be compared in different PW Doppler windows in a synchronous manner;
 - 4) 2-D vector flow dynamics can be acquired over entire regions within a single cardiac cycle (see [32]); and
 - 5) imaging of blood flow and tissue motion in arteries can be performed simultaneously [114].

These features should have a strong impact on examination duration, especially the ability to retrospectively select PW Doppler windows. Also, these factors contribute to a more refined analysis of complex blood flows. In this regard, simultaneous quantification within separate PW Doppler windows is particularly valuable. An example of ultrafast Doppler imaging in the human carotid is presented in Fig. 9.

Beyond these interesting features, the ability of ultrasound to yield a very large amount of new information makes it ideal for detecting very subtle blood flow in small

vessels. Indeed, the ultrafast acquisition of backscattered echoes within a single cardiac cycle dramatically increases the number of temporal samples in each pixel of the blood flow image. This accumulation of data results in the fact that Doppler shows higher sensitivity for slow flow rates (up to 1 mm/s in some applications). So far, it is too soon to predict the possible implications of the extreme sensitivity exhibited by ultrafast Doppler, but potential clinical targets include neovascularization imaging in tumors without the requirement for contrast agents (for example in breast cancer diagnosis or detection of prostate cancer recurrence). These applications, along with other uses, are currently under investigation. In the challenging case of myocardial vascularization, Osmanski *et al.* demonstrated *in vivo* that small vessels can be detected in cardiac muscle without the need to inject contrast agents [115]. In fact, a correction factor based on frequency de-modulation for tissue motion was introduced to analyze this extreme case of a rapidly moving organ. Also, Denarie *et al.* recently studied the influence of frame rate on coherent plane-wave compounding in rapidly moving organs and proposed a correction method for the degradation of

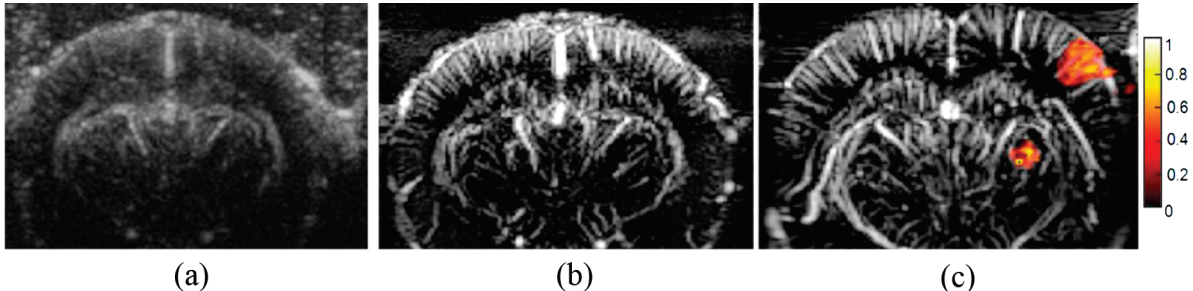


Fig. 10. 2-D maps of the rat cerebral blood volume: (a) using conventional ultrasound Doppler and (b) using ultrafast Doppler. (c) fUS imaging during a task invoked experiment. A mechanical stimulator was employed to excite the whiskers and activation (CBV increase) was clearly detected in the somatosensory cortex and thalamus relay, showing the excellent sensitivity and resolution of fUS imaging (adapted from [119]).

coherent synthetic summation that occurs in these types of organs [116]. Finally, Yu and colleagues recently also used the concept of coherent plane wave compounding for color-encoded speckle and vector Doppler imaging of complex flow dynamics [117].

VIII. ULTRAFAST DOPPLER IMAGING OF BRAIN ACTIVITY: ULTRASOUND

Probably the most fascinating impact of ultrafast imaging has been in neuroscience, because the quest for understanding the human mind has been one of the fundamental desires of humans throughout the ages. Today, neuroscience joins all scientific communities, including biologists, physicists, mathematicians, computer scientists, and philosophers in a common quest to answer questions concerning thoughts, feelings, memories, and other mysterious functions of the human mind. Imaging of the human brain has proven invaluable in this search for knowledge. In the early 1990s, the advent of fMRI revolutionized the understanding of the brain, paving the way for several of the major discoveries of the last decades in neuroscience. It is still advancing and remains the most popular gold-

standard imaging technique available today for deep brain functional imaging. However, recent improvements in deep brain imaging technology have been somewhat limited because they are, for the most part, based on incremental innovation using mature techniques (e.g., EEG, PET, and fMRI) instead of emerging technologies.

The major advantage of fMRI is that functional imaging can be performed deep in the brain with high spatial resolution. It can also be used to measure increases in blood-oxygen level dependent (BOLD) signals when the change in blood flow resulting from neuronal activation exceeds oxygen consumption. However, fMRI suffers from some limitations. In fundamental research, for small animal imaging, very strong magnetic fields are needed to reach high spatial resolutions (i.e., 150 to 300 μm). Moreover, spatially resolved fMRI is achieved at the cost of a substantial drop in temporal resolution and/or signal-to-noise ratio. For this reason, imaging of transient events, such as epilepsy, is particularly challenging. Finally, fMRI is not suited to many clinical applications. Cost, size, and portability of MRI machines can limit patient accessibility. In neonatal pediatric neurology, fMRI is rarely performed because of specific issues concerning practical exam complexity. In neurosurgery, fMRI cannot be performed in the

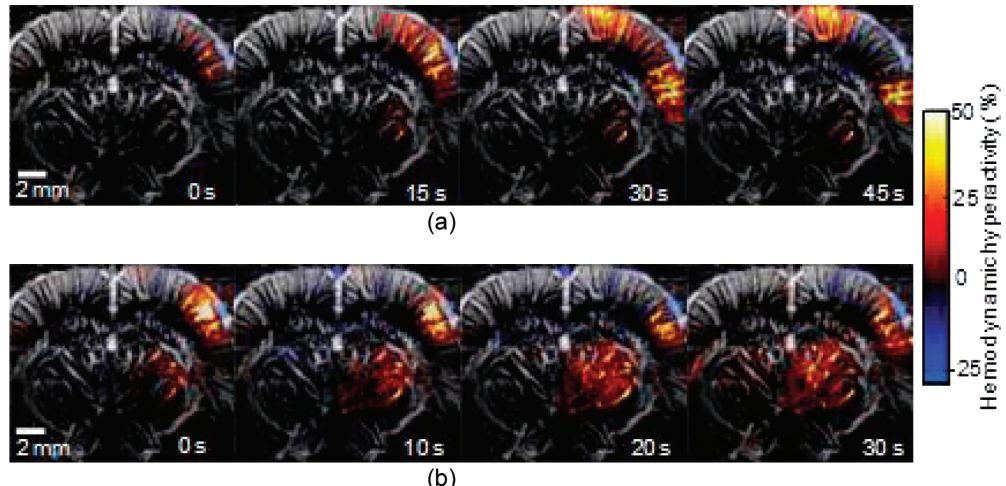


Fig. 11. Spatiotemporal spreading of epileptiform activity for two ictal events. Brain cerebral blood volume (CBV) changes (% relative to the baseline) are superimposed on a control baseline CBV image. In (a) we can see an onset and a cortical propagation. In (b), the activity is seen spreading in the thalamus (adapted from [118]).

operating room for monitoring patient cerebral function. Therefore, there is room for cutting-edge research into the development of new neuro-imaging modalities.

Even though ultrasound is the most widely used modality in clinics for blood flow imaging, it has never played this role in neuroscience. Indeed, ultrasound imaging is not sensitive enough to see low blood flow in small vessels, and is only useful when imaging larger vessels. Recently, our group partially solved this sensitivity problem using ultrafast Doppler, proving that ultrasound can represent an alternative in functional imaging of brain activity [118], [119]. Therefore, for the first time, the huge increase in sensitivity provided by ultrafast Doppler [119] can be used to map subtle hemodynamic changes in brain vascularization [Figs. 10(a) and 10(b)]. For example, use of this technology in the brain could provide new information regarding stroke [120].

Ultrafast Doppler (called μ Doppler) displays very high sensitivity compared with conventional color flow imaging, resulting from both synergetic sensitivity gains resulting from coherent plane-wave compounding [112] and time averaging of the ultrafast accumulated data over large durations [27], [119]. At a given depth (z), the gain in terms of sensitivity for μ Doppler compared with conventional CFI can be written as

$$G_{\mu\text{Doppler}}(z) = \frac{S_{\mu\text{Doppler}}}{S_{\text{CFI}}} = N_{\text{angles}} \frac{\sqrt{\lambda z}}{D} \sqrt{\frac{n_{\text{eff}}^{\mu\text{Doppler}}}{n_{\text{eff}}^{\text{CFI}}}},$$

where $S_{\mu\text{Doppler}}$ and S_{CFI} are the intensities of the Doppler signal in ultrafast Doppler and conventional Doppler, respectively. N_{angles} is the number of angles used for tilted plane-wave transmissions, λ is the wavelength, z is the observation depth, D is the aperture used for transmit focusing in conventional CFI, and $n_{\text{eff}}^{\mu\text{Doppler}}$ and $n_{\text{eff}}^{\text{CFI}}$ are the number of temporal samples available for the Doppler signal at each pixel for ultrafast Doppler and conventional CFI, respectively. In typical configurations at a 15 kHz pulse repetition frequency for rodent imaging, $N_{\text{angles}} = 16$, $D = 4$ mm, $z = 15$ mm, $\lambda = 150$ μm , $n_{\text{eff}}^{\mu\text{Doppler}} = 400$, and $n_{\text{eff}}^{\text{CFI}} = 10$, leading to an almost 2-fold gain: $G_{\mu\text{Doppler}} \approx 38$.

The first *in vivo* proof of this concept was shown by imaging functional changes of cerebral blow volume (CBV) in the microvascularization of trepanned rat brain during whisker stimulation [Fig. 10(c)] or epileptic seizures (Fig. 11), leading to the concept of fUltrasound (by analogy to fMRI).

The fUltrasound technique has many important implications in neuroscience. In basic neuroscience, this unique modality should provide a real-time, portable method of functional deep-brain imaging in awake or freely moving small animals with unprecedented spatiotemporal resolution (~ 100 μm , 50 ms). In clinical diagnosis, it can provide a unique bedside neuro-imaging system for monitoring brain activity of newborns through the fontanel window. Also, this real-time system can enable assessment and study of neonatal seizures and hemorrhages. In adults,

ultrasound provides a unique functional imaging modality during neurosurgery for predicting the remodeling of cortical mapping resulting from tumor development (e.g., low-grade gliomas).

IX. ULTRAFAST ULTRASOUND: BEYOND MEDICAL IMAGING

The concept of ultrafast ultrasound has given rise to new applications beyond medical imaging. First, in fundamental physics, ultrafast frame rates allow for imaging of shock transverse waves at very high Mach numbers (typically > 1) in elastic media [121]. In addition, this technology could contribute to a better understanding of nonlinear wave propagation in solids as well as shocks in humans for road traffic safety. In geophysics, ultrafast scanners were recently used to follow the dynamics of interface failure during friction experiments, and new imaging has revealed the supershear rupture regime associated with the emission of Mach wave fronts. Notably, ultrafast scanners provide a small-scale laboratory setup for making novel geophysical observations that can be translated to the level of the Earth (e.g., slip dynamics in active faults) [122]. Finally, in the field of physical chemistry and rheology, ultrafast scanners are likely to become valuable tools for characterizing soft materials under shear forces, as recently demonstrated by Gallot *et al.* in an unstable shear-banded flow of non-Newtonian wormlike micellar solution [123].

X. CONCLUSIONS

After more than twenty years of extensive research in the field of ultrafast imaging, new ultrasonic imaging modes have emerged, including shear wave elastography, electromechanical wave imaging, ultrafast Doppler, ultrafast contrast imaging, and even functional ultrasound imaging of brain activity (fUltrasound). These modalities can be utilized in both basic research and clinical applications. Notably, this technology has grown exponentially because of developments in GPU technology, which has permitted frame rates of > 1000 frames per second. **Thus, these techniques have surpassed the research phase and are now entering the clinical medical ultrasound community.** Undoubtedly, these ultrafast modes will lead to advancements in prevention, diagnosis, and therapeutic monitoring. Furthermore, beyond radiology, ultrafast-associated technology is already spreading to many other research fields, such as physical chemistry and geophysics.

REFERENCES

- [1] C. Chilowsky and P. Langevin, "Procédés et appareils pour la production de signaux sous-marins dirigés et pour la localisation à distance d'obstacles sous-marins," French Patent 502913, Mar. 4, 1920.

- [2] T. Szabo, *Diagnostic Ultrasound Imaging: Inside Out*. New York, NY: Elsevier Academic, 2004.
- [3] D. Gabor, "A new microscopic principle," *Nature*, vol. 161, no. 4098, pp. 777–778, May 1948.
- [4] M. Fink, C. Prada, F. Wu, and D. Cassereau, "Self focusing in inhomogeneous media with time reversal acoustic mirrors," in *Proc. IEEE Ultrasonics Symp.*, 1989, pp. 681–686.
- [5] M. Fink, "Time reversal of ultrasonic fields: 1. Basic Principles," *IEEE Trans. Ultrason. Ferroelectr. Freq. Control*, vol. 39, no. 5, pp. 555–566, 1992.
- [6] M. Fink, G. Montaldo, and M. Tanter, "Time-reversal acoustics in biomedical engineering," *Annu. Rev. Biomed. Eng.*, vol. 5, pp. 465–497, 2003.
- [7] C. Bruneel, R. Torguet, K. M. Rouvain, E. Bridoux, and B. Non-gaillard, "Ultrafast echotomographic system using optical processing of ultrasonic signals," *Appl. Phys. Lett.*, vol. 30, no. 8, pp. 371–373, 1977.
- [8] B. Delannoy, R. Torguet, C. Bruneel, E. Bridoux, J. M. Rouaven, and H. Lasota, "Acoustical image reconstruction in parallel-processing analog electronic systems," *J. Appl. Phys.*, vol. 50, no. 5, pp. 3153–3159, 1979.
- [9] M. Couade, M. Pernot, M. Tanter, E. Messas, A. Bel, M. Ba, A.-A. Hagege, and M. Fink, "Ultrafast imaging of the heart using circular wave synthetic imaging with phased arrays," in *IEEE Int. Ultrasonics Symp.*, 2009, pp. 515–518.
- [10] D. Shattuck, M. Weishenker, S. Smith, and O. von Ramm "Exploscan: A parallel processing technique for high speed ultrasound imaging with linear phased arrays," *J. Acoust. Soc. Am.*, vol. 75, no. 4, pp. 1273–1282, Apr. 1984.
- [11] S. W. Smith, H. G. Pavay Jr., and O. T. von Ramm, "High-speed ultrasound volumetric imaging system. I. Transducer design and beam steering," *IEEE Trans. Ultrason. Ferroelectr. Freq. Control*, vol. 38, no. 2, pp. 100–108, Mar. 1991.
- [12] O. T. von Ramm, S. W. Smith, and H. G. Pavay Jr., "High-speed ultrasound volumetric imaging system. II. Parallel processing and image display," *IEEE Trans. Ultrason. Ferroelectr. Freq. Control*, vol. 38, no. 2, pp. 109–115, 1991.
- [13] M. Fink, "Ultrasound imaging," *Rev. Phys. Appl.*, vol. 18, no. 9, pp. 527–556, 1983.
- [14] M. Fink, D. Cassereau, A. Derode, C. Prada, P. Roux, M. Tanter, J.-L. Thomas, and F. Wu, "Time-reversed acoustics," *Rep. Prog. Phys.*, vol. 63, no. 12, pp. 1933–1995, 2000.
- [15] L. Sandrin, S. Catheline, M. Tanter, X. Hennequin, and M. Fink, "Time-resolved pulsed elastography with ultrafast ultrasonic imaging," *Ultrason. Imaging*, vol. 21, no. 4, pp. 259–272, 1999.
- [16] M. Tanter, J. Bercoff, L. Sandrin, and M. Fink, "Ultrafast compound imaging for 2-D motion vector estimation: Application to transient elastography," *IEEE Trans. Ultrason. Ferroelectr. Freq. Control*, vol. 49, no. 10, pp. 1363–1374, 2002.
- [17] L. Sandrin, M. Tanter, S. Catheline, and M. Fink, "Shear modulus imaging with 2-D transient elastography," *IEEE Trans. Ultrason. Ferroelectr. Freq. Control*, vol. 49, no. 4, pp. 426–435, 2002.
- [18] J. Bercoff, S. Chaffai, M. Tanter, L. Sandrin, S. Catheline, M. Fink, J. L. Gennisson, and M. Meunier, "In vivo breast tumor detection using transient elastography," *Ultrasound Med. Biol.*, vol. 29, no. 10, pp. 1387–1396, 2003.
- [19] J.-Y. Lu and J. F. Greenleaf, "Pulse-echo imaging using a non-diffracting beam transducer," *Ultrasound Med. Biol.*, vol. 17, pp. 265–281, May 1991.
- [20] J.-Y. Lu and J. F. Greenleaf, "Ultrasonic nondiffracting transducer for medical imaging," *IEEE Trans. Ultrason. Ferroelectr. Freq. Control*, vol. 37, pp. 438–447, Sep. 1990.
- [21] J.-Y. Lu and J. F. Greenleaf, "Experimental verification of nondiffracting X waves," *IEEE Trans. Ultrason. Ferroelectr. Freq. Control*, vol. 39, pp. 441–446, May 1992.
- [22] J.-Y. Lu, "2-D and 3-D high frame rate imaging with limited diffraction beams," *IEEE Trans. Ultrason. Ferroelectr. Freq. Control*, vol. 44, pp. 839–856, Jul. 1997.
- [23] J.-Y. Lu, "Experimental study of high frame rate imaging with limited diffraction beams," *IEEE Trans. Ultrason. Ferroelectr. Freq. Control*, vol. 45, pp. 84–97, Jan. 1998.
- [24] J. Cheng and J.-Y. Lu, "Extended high frame rate imaging method with limited diffraction beams," *IEEE Trans. Ultrason. Ferroelectr. Freq. Control*, vol. 53, pp. 880–899, May 2006.
- [25] M. Pernot, M. Tanter, J. Bercoff, K. R. Waters, and M. Fink, "Temperature estimation using ultrasonic spatial compound imaging," *IEEE Trans. Ultrason. Ferroelectr. Freq. Control*, vol. 51, no. 5, pp. 606–615, 2004.
- [26] M. Tanter, J. Bercoff, A. Athanasiou, T. Deffieux, J.-L. Gennisson, G. Montaldo, M. Muller, A. Tardivon, and M. Fink, "Quantitative assessment of breast lesion viscoelasticity: Initial clinical results using supersonic shear imaging," *Ultrasound Med. Biol.*, vol. 34, no. 9, pp. 1373–1386, 2008.
- [27] G. Montaldo, M. Tanter, J. Bercoff, N. Benech, and M. Fink, "Coherent plane-wave compounding for very high frame rate ultrasonography and transient elastography," *IEEE Trans. Ultrason. Ferroelectr. Freq. Control*, vol. 56, no. 3, pp. 489–506, 2009.
- [28] C. R. Cooley and B. S. Robinson, "Synthetic focus imaging using partial datasets," in *Proc. IEEE Ultrasonics Symp.*, 1994, vol. 3, pp. 1539–1542.
- [29] S. I. Nikolov and J. A. Jensen, "In-vivo synthetic aperture flow imaging in medical ultrasound," *IEEE Trans. Ultrason. Ferroelectr. Freq. Control*, vol. 50, no. 7, pp. 848–856, 2003.
- [30] S. I. Nikolov and J. A. Jensen, "K-space model of motion artifacts in synthetic transmit ultrasound imaging," in *IEEE Symp. Ultrasonics*, 2003, p. 1824.
- [31] N. Oddershede and J. Jensen, "Effects influencing focusing in synthetic aperture vector flow imaging," *IEEE Trans. Ultrason. Ferroelectr. Freq. Control*, vol. 54, pp. 1811–1825, Sep. 2007.
- [32] J. Udesen, F. Gran, K. L. Hansen, J. A. Jensen, C. Thomsen, and M. B. Nielsen, "High frame-rate blood vector velocity imaging using plane waves: Simulations and preliminary experiments," *IEEE Trans. Ultrason. Ferroelectr. Freq. Control*, vol. 55, no. 8, pp. 1729–1743, 2008.
- [33] S. I. Nikolov, J. Kortbek, and J. A. Jensen, "Practical applications of synthetic aperture imaging," in *IEEE Int. Ultrasonics Symp.*, 2010, pp. 350–358.
- [34] S. I. Nikolov, "Synthetic aperture tissue and flow ultrasound imaging," Ph.D. dissertation, Dept. of Biomedical Engineering, Ørsted-DTU, Technical University of Denmark, Lyngby, Denmark, 2001.
- [35] G. R. Lockwood, J. R. Talman, and S. S. Brunke, "Real-time 3D ultrasound imaging using sparse synthetic aperture beamforming," *IEEE Trans. Ultrason. Ferroelectr. Freq. Control*, vol. 45, no. 4, pp. 980–988, 1998.
- [36] C. R. Hazard and G. R. Lockwood, "Theoretical assessment of a synthetic aperture beamformer for real-time 3-D imaging," *IEEE Trans. Ultrason. Ferroelectr. Freq. Control*, vol. 46, no. 4, pp. 972–980, 1999.
- [37] M. Karaman, P. C. Li, and M. O'Donnell, "Synthetic aperture imaging for small scale systems," *IEEE Trans. Ultrason. Ferroelectr. Freq. Control*, vol. 42, no. 3, pp. 429–442, 1995.
- [38] S. I. Nikolov and J. A. Jensen, "Virtual ultrasound sources in high-resolution ultrasound imaging," in *Proc. SPIE*, 2002, vol. 3, pp. 395–405.
- [39] L. Y. L. Mo, D. Napolitano, G. W. McLaughlin, and D. DeBusschere, "Zone-based color flow imaging," in *Proc. IEEE Ultrasonics Symp.*, 2003, pp. 29–32.
- [40] D. Napolitano, G. W. McLaughlin, D. DeBusschere, and L. Y. L. Mo, "Zone-based B-mode imaging," in *Proc. IEEE Ultrasonics Symp.*, 2003, pp. 25–28.
- [41] K. Owen, M. I. Fuller, and J. A. Hossack, "Application of x-y separable 2-D array beamforming for increased frame rate and energy efficiency in handheld devices," *IEEE Trans. Ultrason. Ferroelectr. Freq. Control*, vol. 59, no. 7, pp. 1332–1343, 2012.
- [42] S. Park, S. R. Aglyamov, and S. Y. Emelianov, "Elasticity Imaging using conventional and high-frame rate ultrasound imaging: Experimental study," *IEEE Trans. Ultrason. Ferroelectr. Freq. Control*, vol. 54, no. 11, pp. 2246–2256, 2007.
- [43] J. Y. Lu, J. Q. Cheng, and J. Wang, "High frame rate imaging system for limited diffraction array beam imaging with square-wave aperture weightings," *IEEE Trans. Ultrason. Ferroelectr. Freq. Control*, vol. 53, no. 10, pp. 1796–1812, 2006.
- [44] A. Geist "Paving the roadmap to exascale," *SciDAC Rev.*, no. 16, special issue, pp. 52–59, 2010.
- [45] R. Muthupillai, D. J. Lomas, P. J. Rossman, J. F. Greenleaf, A. Manduca, and R. L. Ehman, "Magnetic resonance elastography by direct visualization of propagating acoustic strain wave," *Science*, vol. 269, pp. 1854–1857, 1995.
- [46] R. Sinkus, M. Tanter, T. Xydeas, S. Catheline, J. Bercoff, and M. Fink, "Viscoelastic shear properties of in vivo breast lesions measured by MR elastography," *Magn. Res. Imaging*, vol. 23, no. 2, pp. 159–165, 2005.

- [47] K. J. Parker and R. M. Lerner, "Sonoelasticity of organs: Shear waves ring a bell," *J. Ultrasound Med.*, vol. 11, no. 8, pp. 387–392, 1992.
- [48] A. P. Sarvazyan, O. V. Rudenko, S. D. Swanson, J. B. Fowlkes, and S. Y. Emelianov, "Shear wave elasticity imaging—A new ultrasonic technology of medical diagnostics," *Ultrasound Med. Biol.*, vol. 24, no. 9, pp. 1419–1436, 1998.
- [49] K. Nightingale, M. S. Soo, R. Nightingale, and G. Trahey, "Acoustic radiation force impulse imaging: In vivo demonstration of clinical feasibility," *Ultrasound Med. Biol.*, vol. 28, no. 2, pp. 227–235, 2002.
- [50] M. L. Palmeri, M. H. Wang, J. J. Dahl, K. D. Frinkley, and K. R. Nightingale, "Quantifying hepatic shear modulus in vivo using acoustic radiation force," *Ultrasound Med. Biol.*, vol. 34, no. 4, pp. 546–558, 2008.
- [51] J. Bercoff, M. Tanter, and M. Fink, "Supersonic shear imaging: A new technique for soft tissue elasticity mapping," *IEEE Trans. Ultrason. Ferroelectr. Freq. Control*, vol. 51, no. 4, pp. 396–409, 2004.
- [52] J. Bercoff, M. Tanter, and M. Fink, "Sonic boom in soft materials: The elastic Cerenkov effect," *Appl. Phys. Lett.*, vol. 84, no. 12, pp. 2202–2204, 2004.
- [53] J. R. Doherty, G. E. Trahey, K. R. Nightingale, and M. L. Palmeri, "Acoustic radiation force elasticity imaging in diagnostic ultrasound," *IEEE Trans. Ultrason. Ferroelectr. Freq. Control*, vol. 60, no. 4, pp. 685–701, 2013.
- [54] M. H. Wang, M. L. Palmeri, V. M. Rotemberg, N. C. Rouze, and K. R. Nightingale, "Improving the robustness of time-of-flight shear wave speed reconstruction methods using RANSAC in human liver in vivo," *Ultrasound Med. Biol.*, vol. 36, no. 5, pp. 802–813, 2010.
- [55] M. Fink and M. Tanter, "Multiwave imaging and super resolution," *Phys. Today*, vol. 63, no. 2, pp. 28–33, 2010.
- [56] A. Athanasiou, A. Tardivon, M. Tanter, B. Sigal-Zafrani, J. Bercoff, T. D. Eux, J.-L. Gennisson, M. Fink, and S. Neuenschwander, "Breast lesions: Quantitative elastography with supersonic shear imaging—Preliminary results," *Radiology*, vol. 256, no. 1, pp. 297–303, 2010.
- [57] W. A. Berg, D. O. Cosgrove, C. J. Doré, F. K. Schäfer, W. E. Svensson, R. J. Hooley, R. Ohlinger, E. B. Mendelson, C. Balu-Maestro, M. Locatelli, C. Tourasse, B. C. Cavanaugh, V. Juhan, A. T. Stavros, A. Tardivon, J. Gay, J. P. Henry, and C. Cohen-Bacrie, "Shear-wave elastography improves the specificity of breast US: The BE1 multinational study of 939 masses," *Radiology*, vol. 262, no. 2, pp. 435–449, 2012.
- [58] T. Deffieux, G. Montaldo, M. Tanter, and M. Fink, "Shear wave spectroscopy for in vivo quantification of human soft tissues viscoelasticity," *IEEE Trans. Med. Imaging*, vol. 28, no. 3, pp. 313–322, 2009.
- [59] M. Muller, J.-L. Gennisson, T. Deffieux, M. Tanter, and M. Fink, "Quantitative viscoelasticity mapping of human liver using supersonic shear imaging: Preliminary in vivo feasibility study," *Ultrasound Med. Biol.*, vol. 35, no. 2, pp. 219–229, 2009.
- [60] E. Bavu, J.-L. Gennisson, M. Couade, J. Bercoff, V. Mallet, M. Fink, A. Badel, A. Vallet-Pichard, B. Nalpas, M. Tanter, and S. Pol, "Noninvasive in vivo liver fibrosis evaluation using supersonic shear imaging: A clinical study on 113 hepatitis c virus patients," *Ultrasound Med. Biol.*, vol. 37, no. 9, pp. 1361–1373, 2011.
- [61] T. Deffieux, J.-L. Gennisson, M. Tanter, and M. Fink, "Assessment of the mechanical properties of the musculoskeletal system using 2-D and 3-D very high frame rate ultrasound," *IEEE Trans. Ultrason. Ferroelectr. Freq. Control*, vol. 55, no. 10, pp. 2177–2190, 2008.
- [62] M. Shinohara, K. Sabra, J.-L. Gennisson, M. Fink, and M. Tanter, "Real-time visualization of muscle stiffness distribution with ultrasound shear wave imaging during muscle contraction," *Muscle Nerve*, vol. 42, no. 3, pp. 438–441, 2010.
- [63] J.-L. Gennisson, T. Deffieux, E. Mace, G. Montaldo, M. Fink, and M. Tanter, "Viscoelastic and anisotropic mechanical properties of in vivo muscle tissue assessed by supersonic shear imaging," *Ultrasound Med. Biol.*, vol. 36, no. 5, pp. 789–801, 2010.
- [64] M. Couade, M. Pernot, C. Prada, E. Messas, J. Emmerich, P. Bruneval, A. Criton, M. Fink, and M. Tanter, "Quantitative assessment of arterial wall biomechanical properties using shear wave imaging," *Ultrasound Med. Biol.*, vol. 36, no. 10, pp. 1662–1676, 2010.
- [65] M. Couade, M. Pernot, E. Messas, A. Bel, M. Ba, A. Hagege, M. Fink, and M. Tanter, "In vivo quantitative mapping of myocardial stiffening and transmural anisotropy during the cardiac cycle," *IEEE Trans. Med. Imaging*, vol. 30, no. 2, pp. 295–305, 2011.
- [66] M. Pernot, M. Couade, P. Mateo, B. Crozatier, R. Fischmeister, and M. Tanter, "Real-time assessment of myocardial contractility using shear wave imaging," *J. Am. Coll. Cardiol.*, vol. 58, no. 1, pp. 65–72, 2011.
- [67] M. Tanter, D. Touboul, J.-L. Gennisson, J. Bercoff, and M. Fink, "High-resolution quantitative imaging of cornea elasticity using supersonic shear imaging," *IEEE Trans. Med. Imaging*, vol. 28, no. 12, pp. 1881–1893, 2009.
- [68] J. Bercoff, M. Pernot, M. Tanter, and M. Fink, "Monitoring thermally-induced lesions with supersonic shear imaging," *Ultrason. Imaging*, vol. 26, no. 2, pp. 71–84, 2004.
- [69] B. Arnal, M. Pernot, and M. Tanter, "Monitoring of thermal therapy based on shear modulus changes: II. Shear wave imaging of thermal lesions," *IEEE Trans. Ultrason. Ferroelectr. Freq. Control*, vol. 58, no. 8, pp. 1603–1611, 2011.
- [70] T. Y. Wang, T. L. Hall, Z. Xu, J. B. Fowlkes, and C. A. Cain, "Imaging feedback of histotripsy treatments using ultrasound shear wave elastography," *IEEE Trans. Ultrason. Ferroelectr. Freq. Control*, vol. 59, no. 6, pp. 1167–1181, 2012.
- [71] E. Sapin-de Brosses, M. Pernot, and M. Tanter, "The link between tissue elasticity and thermal dose in vivo," *Phys. Med. Biol.*, vol. 56, no. 24, pp. 7755–7765, 2011.
- [72] P. Song, H. Zhao, A. Manduca, M. W. Urban, J. F. Greenleaf, and S. G. Chen, "Comb-push ultrasound shear elastography (CUSE): A novel method for two-dimensional shear elasticity imaging of soft tissues," *IEEE Trans. Med. Imaging*, vol. 31, no. 9, pp. 1821–1832, 2012.
- [73] H. Kanai and Y. Koiwa, "Myocardial rapid velocity distribution," *Ultrasound Med. Biol.*, vol. 27, no. 4, pp. 481–498, 2001.
- [74] Y. Koiwa, H. Kanai, H. Hasegawa, Y. Saitoh, and K. Shirato, "Left ventricular transmural systolic function by high-sensitivity velocity measurement 'phased-tracking method' across the septum in doxorubicin cardiomyopathy," *Ultrasound Med. Biol.*, vol. 28, no. 11–12, pp. 1395–1403, 2002.
- [75] H. Kanai, "Propagation of spontaneously actuated pulsive vibration in human heart wall and in vivo viscoelasticity estimation," *IEEE Trans. Ultrason. Ferroelectr. Freq. Control*, vol. 52, no. 11, pp. 1931–1942, 2005.
- [76] M. Pernot and E. Konofagou, "Electromechanical imaging of the myocardium at normal and pathological states," in *Proc. IEEE Int. Ultrasonics Symp.*, 2005, pp. 1091–1094.
- [77] M. Pernot, K. Fujikura, S. D. Fung-Kee-Fung, and E. Konofagou, "ECG-gated, mechanical and electromechanical wave imaging of cardiovascular tissues in vivo," *Ultrasound Med. Biol.*, vol. 33, no. 7, pp. 1075–1085, 2007.
- [78] E. Konofagou, J. Luo, D. Saluja, D. O. Cervantes, J. Coronillas, and K. Fujikura, "Noninvasive electromechanical wave imaging and conduction velocity estimation in vivo," in *Proc. IEEE Ultrasonics Symp.*, 2007, pp. 969–972.
- [79] T. Deffieux, J.-L. Gennisson, M. Tanter, M. Fink, and A. Nordez, "Ultrafast imaging of in vivo muscle contraction using ultrasound," *Appl. Phys. Lett.*, vol. 89, no. 18, art. no. 184107, 2006.
- [80] J. Provost, W.-N. Lee, K. Fujikura, and E. E. Konofagou, "Electromechanical wave imaging of normal and ischemic hearts in vivo," *IEEE Trans. Med. Imaging*, vol. 29, no. 3, pp. 625–635, Mar. 2010.
- [81] E. Konofagou, W.-N. Lee, J. Luo, J. Provost, and J. Vappou, "Physiologic cardiovascular strain and intrinsic wave imaging," *Annu. Rev. Biomed. Eng.*, vol. 13, pp. 477–505, 2011.
- [82] S. Wang, W.-N. Lee, J. Provost, J. Luo, and E. E. Konofagou, "A composite high-frame-rate system for clinical cardiovascular imaging," *IEEE Trans. Ultrason. Ferroelectr. Freq. Control*, vol. 55, no. 10, pp. 2221–2233, 2008.
- [83] J. Provost, W.-N. Lee, K. Fujikura, and E. E. Konofagou, "Imaging the electromechanical activity of the heart in vivo," *Proc. Natl. Am. Soc.*, vol. 108, no. 21, pp. 8565–8570, 2011.
- [84] H. Kanai, "Propagation of vibration caused by electrical excitation in the normal human heart," *Ultrasound Med. Biol.*, vol. 35, no. 6, pp. 936–948, 2009.
- [85] J. Provost, S. Thiebaut, J. Luo, and E. E. Konofagou, "Single-heartbeat electromechanical wave imaging using temporally unequally spaced acquisition sequences," *Phys. Med. Biol.*, vol. 57, no. 4, pp. 1095–1112, 2012.
- [86] J. Provost, A. Gambhir, J. Vest, H. Garan, and E. E. Konofagou, "A clinical feasibility study of atrial and ventricular electromechanical wave imaging," *Heart Rhythm*, vol. 10, no. 6, pp. 856–862, 2013.
- [87] Y. C. Fung, *Biomechanics: Mechanical Properties of Living Tissues*. New York, NY: Springer-Verlag, 1993.

- [88] R. Asmar, A. Benetos, J. Topouchian, P. Laurent, B. Pannier, A. M. Brisac, R. Target, and B. I. Levy, "Assessment of arterial distensibility by automatic pulse-wave velocity measurement—Validation and clinical application studies," *Hypertension*, vol. 26, no. 3, pp. 485–490, 1995.
- [89] H. Hasegawa and H. Kanai, "Simultaneous imaging of artery-wall strain and blood flow by high frame rate acquisition of RF signals," *IEEE Trans. Ultrason. Ferroelectr. Freq. Control*, vol. 55, no. 12, pp. 2626–2639, 2008.
- [90] J. Vappou, J. W. Luo, and E. E. Konofagou, "Pulse wave imaging for noninvasive and quantitative measurement of arterial stiffness in vivo," *Am. J. Hypertens.*, vol. 23, no. 4, pp. 393–398, 2010.
- [91] M. Couade, M. Pernot, E. Messas, J. Emmerich, A. Hagege, M. Fink, and M. Tanter, "Ultrafast imaging of the arterial pulse wave," *IRBM*, vol. 32, no. 2, pp. 106–108, 2011.
- [92] J. Luo, R. X. Li, and E. E. Konofagou, "Pulse wave imaging of the human carotid artery: An in vivo feasibility study," *IEEE Trans. Ultrason. Ferroelectr. Freq. Control*, vol. 59, no. 1, pp. 174–181, 2012.
- [93] K. Wei, "Contrast echocardiography: Applications and limitations," *Cardiol. Rev.*, vol. 20, no. 1, pp. 25–32, 2012.
- [94] S. R. Wilson and P. N. Burns, "Microbubble-enhanced US in body imaging: What role?" *Radiology*, vol. 257, no. 1, pp. 24–39, 2010.
- [95] J. R. Lindner, "Molecular imaging of cardiovascular disease with contrast-enhanced ultrasonography," *Nature Rev. Cardiol.*, vol. 6, no. 7, pp. 475–481, 2009.
- [96] I. Tardy, S. Pochon, M. Theraulaz, P. Emmel, L. Passantino, F. Tranquart, and M. Schneider, "Ultrasound molecular imaging of VEGFR2 in a rat prostate tumor model using BR55," *Invest. Radiol.*, vol. 45, no. 10, pp. 573–578, 2010.
- [97] P. D. Bevan, R. Kashaffian, E. G. Tickner, and P. N. Burns, "Quantitative measurement of ultrasound disruption of polymer-shelled microbubbles," *Ultrasound Med. Biol.*, vol. 33, no. 11, pp. 1777–1786, 2007.
- [98] W. S. Chen, T. J. Matula, and L. A. Crum, "The disappearance of ultrasound contrast bubbles: Observations of bubble dissolution and cavitation nucleation," *Ultrasound Med. Biol.*, vol. 28, no. 6, pp. 793–803, 2002.
- [99] O. Couture, S. Bannouf, G. Montaldo, J.-F. Aubry, M. Fink, and M. Tanter, "Ultrafast imaging of ultrasound contrast agents," *Ultrasound Med. Biol.*, vol. 35, no. 11, pp. 1908–1916, 2009.
- [100] A. Bouakaz, P. J. A. Frinking, N. de Jong, and N. Bom, "Non-invasive measurement of the hydrostatic pressure in a fluid-filled cavity based on the disappearance time of micrometer-sized free gas bubbles," *Ultrasound Med. Biol.*, vol. 25, no. 9, pp. 1407–1415, 1999.
- [101] O. Couture, M. Faivre, N. Pannacci, A. Babataheri, V. Servois, P. Tabeling, and M. Tanter, "Ultrasound internal tattooing," *Med. Phys.*, vol. 38, no. 2, pp. 1116–1123, 2011.
- [102] O. Couture, A. Urban, A. Bretagne, L. Martinez, M. Tanter, and P. Tabeling, "In vivo targeted delivery of large payloads with an ultrasound clinical scanner," *Med. Phys.*, vol. 39, no. 8, pp. 5229–5237, 2012.
- [103] J. Gateau, J.-F. Aubry, D. Chauvet, A.-L. Boch, M. Fink, and M. Tanter, "In vivo bubble nucleation probability in sheep brain tissue," *Phys. Med. Biol.*, vol. 56, no. 22, pp. 7001–7015, Nov. 2011.
- [104] J. Gateau, J.-F. Aubry, M. Pernot, M. Fink, and M. Tanter, "Combined passive detection and ultrafast active imaging of cavitation events induced by short pulses of high-intensity ultrasound," *IEEE Trans. Ultrason. Ferroelectr. Freq. Control*, vol. 58, no. 3, pp. 517–532, 2011.
- [105] Y. Desailly, O. Couture, M. Fink, and M. Tanter, "Sono-activated ultrasound localization microscopy," *Appl. Phys. Lett.*, vol. 103, no. 17, art. no. 174107, 2013.
- [106] J. E. Thomas, P. Dayton, D. May, and K. Ferrara, "Threshold of fragmentation for ultrasonic contrast agents," *J. Biomed. Opt.*, vol. 6, no. 2, pp. 141–150, 2001.
- [107] O. Couture, M. Fink, and M. Tanter, "Ultrasound contrast plane wave imaging," *IEEE Trans. Ultrason. Ferroelectr. Freq. Control*, vol. 59, no. 12, pp. 2676–2683, 2012.
- [108] O. Couture, E. Dransart, S. Dehay, F. Nemati, D. Decaudin, L. Johannes, and M. Tanter, "Tumor delivery of ultrasound contrast agents using Shiga toxin B subunit," *Mol. Imaging*, vol. 10, no. 2, pp. 135–143, 2011.
- [109] D. H. Evans, W. N. McDicken, R. Skidmore, and J. P. Woodcock, *Doppler Ultrasound, Physics, Instrumentation, and Clinical Applications*. New York, NY: Wiley, 1989.
- [110] J. A. Jensen, *Estimation of Blood Velocities Using Ultrasound: A Signal Processing Approach*. New York, NY: Cambridge University Press, 1996.
- [111] L. Forzoni, D. Righi, G. Ciuti, S. Morovic, I. Zavoreo, F. Mecacci, C. Bussadori, and P. Tortoli, "Multigate quality Doppler profiles technology in vascular, obstetrics and cardiology applications," *Biomed. Tech. (Berlin)*, vol. 57, no. 1, pp. 198–201, Sep. 2012.
- [112] J. Bercoff, G. Montaldo, T. Loupas, D. Savery, F. Meziere, M. Fink, and M. Tanter, "Ultrafast compound Doppler imaging: Providing full blood flow characterization," *IEEE Trans. Ultrason. Ferroelectr. Freq. Control*, vol. 58, no. 1, pp. 134–147, 2011.
- [113] K. L. Hansen, J. Udesen, F. Gran, J. A. Jensen, and M. B. Nielsen, "In-vivo examples of flow patterns with the fast vector velocity ultrasound method," *Ultraschall Med.*, vol. 30, no. 5, pp. 471–477, 2009.
- [114] I. K. Ekroll, A. Swillens, P. Segers, T. Dahl, H. Torp, and L. Lovstakken, "Simultaneous quantification of flow and tissue velocities based on multi-angle plane wave imaging," *IEEE Trans. Ultrason. Ferroelectr. Freq. Control*, vol. 60, no. 4, pp. 727–738, 2013.
- [115] B. F. Osmanski, M. Pernot, G. Montaldo, A. Bel, E. Messas, and M. Tanter, "Ultrafast Doppler imaging of blood flow dynamics in the myocardium," *IEEE Trans. Med. Imaging*, vol. 31, no. 8, pp. 1661–1668, 2012.
- [116] B. Denarie, T. A. Tangen, I. K. Ekroll, N. Rolim, H. Torp, T. Bjastad, and L. Lovstakken, "Coherent plane wave compounding for very high frame rate ultrasonography of rapidly moving targets," *IEEE Trans. Med. Imaging*, vol. 32, no. 7, pp. 1265–1276, 2013.
- [117] B. Y. S. Yiu and A. C. H. Yu, "High frame rate ultrasound color-encoded speckle imaging of complex flow dynamics," *Ultrasound Med. Biol.*, vol. 39, no. 6, pp. 1015–1025, 2013.
- [118] E. Mace, G. Montaldo, I. Cohen, M. Baulac, M. Fink, and M. Tanter, "Functional ultrasound imaging of the brain," *Nat. Methods*, vol. 8, no. 8, pp. 662–664, 2011.
- [119] E. Mace, G. Montaldo, B. F. Osmanski, I. Cohen, M. Fink, and M. Tanter, "Functional ultrasound imaging of the brain: Theory and basic principles," *IEEE Trans. Ultrason. Ferroelectr. Freq. Control*, vol. 60, no. 3, pp. 492–506, 2013.
- [120] A. Martin, E. Mace, R. Boisgard, G. Montaldo, B. Theze, M. Tanter, and B. Tavitian, "Imaging of perfusion, angiogenesis, and tissue elasticity after stroke," *J. Cereb. Blood Flow Metab.*, vol. 32, no. 8, pp. 1496–1507, 2012.
- [121] S. Catheline, J.-L. Gennisson, M. Tanter, and M. Fink, "Observation of shock transverse waves in elastic media," *Phys. Rev. Lett.*, vol. 91, no. 16, p. 164301 2003.
- [122] S. Latour, T. Gallot, S. Catheline, C. Voisin, F. Renard, E. Larose, and M. Campillo, "Ultrafast ultrasonic imaging of dynamic sliding friction in soft solids: The slow slip and the super-shear regimes," *Europhys. Lett.*, vol. 96, no. 5, art. no. 59003, 2011.
- [123] T. Gallot, C. Perge, V. Grenard, M. A. Fardin, N. Taberlet, and S. Manneville, "Ultrafast ultrasonic imaging coupled to rheometry: Principle and illustration," *Rev. Sci. Instrum.*, vol. 84, no. 4, art. no. 045107, 2013.

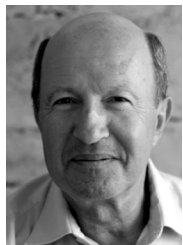


Mickaël Tanter is a Research Professor at the French National Institute for Health and Medical Research (INSERM). For eight years, he has headed Inserm laboratory U979 "Wave Physics for Medicine" at the Langevin Institute, ESPCI Paris, France.

His main activities are centered on the development of new approaches in wave physics for medical imaging and therapy. His current research interests include a wide range of topics: elastography using supersonic shear wave imaging, ultrafast ultrasound imaging, HIFU, and, more recently, the concept of fUltrasound (functional ultrasonic imaging of brain activity). He is the recipient of 24 world patents in the field of ultrasound and the author of more than 160 peer-reviewed papers and book chapters.

M. Tanter is an Associate Editor of the *IEEE Transactions on Ultrasonics, Ferroelectrics, and Frequency Control*, and a member of the technical program committee of the IEEE International Ultrasonics Symposium and administrative committee of IEEE UFFC Society. In 2006, he co-founded Supersonic Imagine with M. Fink, J. Souquet, and C. Cohen-Bacrie. Supersonic Imagine is an innovative French company positioned in the field of medical ultrasound imaging and therapy; in

2009, the company launched a revolutionary ultrafast ultrasound imaging platform, called Aixplorer, with a unique real-time shear wave imaging modality for cancer diagnosis. Supersonic Imagine has more than 120 employees, 102 M€ venture capital, and has already sold more than 750 ultrasound systems worldwide. He has received ten scientific awards, including the Frederic Lizzi Early Career Award of the International Society of Therapeutic Ultrasound, the Montgolfier Prize of the French National Society for Industry Valorization, the Leon Brillouin Prize of the Institute of Electrical and Electronics Engineers (IEEE) and SEE society, the Yves Rocard prize of the French Society of Physics (SFP), the Sylvia Sorkin Greenfield Award of the American Association of Physicists in Medicine for the best paper published in Medical Physics in 2011, the Grand Prize of Medicine and Medical Research of the City of Paris, and the honored lecture of the Radiology Society of North America in 2012. He was recently awarded a prestigious European Research Council (ERC) Advanced Grant to develop fUltrasound applications.



Mathias Fink received the Ph.D. degree in solid-state physics from Paris University in 1970. He then moved to medical imaging and received the Doctorat es-Sciences degree in 1978 from Paris University. His Doctorat es-Sciences research was in the area of ultrasonic focusing with transducer arrays for real-time medical imaging.

Mathias Fink is a professor of physics at the Ecole Supérieure de Physique et de Chimie Industrielles de la Ville de Paris (ESPCI ParisTech),

Paris, France. In 1990, he founded the Laboratory Ondes et Acoustique at ESPCI that became, in 2009, the Langevin Institute. In 2002, he was elected to the French Academy of Engineering, in 2003 to the French Academy of Science, and in 2008 to the Collège de France on the Chair of Technological Innovation. Recently, he received the first CNRS Medal of Innovation, the Rayleigh Award from the IEEE UFFC Society, and the Ian Donald Medal from the International Society of Ultrasound in Obstetrics and Gynecology.

Mathias Fink's area of research is concerned with the propagation of waves in complex media and the development of numerous instruments based on this basic research. His current research interests include time-reversal in physics, super-resolution, metamaterials, medical ultrasonic imaging, ultrasonic therapy, multiwave imaging, acoustic smart objects, acoustic tactile screens, underwater acoustics, geophysics, and telecommunications. He has developed different techniques in medical imaging (ultrafast ultrasonic imaging, transient elastography, and supersonic shear imaging), wave control, and focusing in complex media with time-reversal mirrors. He holds more than 55 patents and he has published more than 350 peer-reviewed papers and book chapters. Four start-up companies have been created from his research (Echosens, Sensitive Object, Supersonic Imagine, and Time Reversal Communications)